FRAMEWORK FOR A FIBRIN-SPECIFIC APTAMER FOR TARGETED DELIVERY OF FIBRINOLYTIC ESCHERICHIA COLI

A Thesis
Presented to
The Academic Faculty

By

Matthew White

In Partial Fulfillment
of the Requirements for the Degree
Master of Science in the
College of Engineering
Wallace H. Coulter Department of Biomedical Engineering

Georgia Institute of Technology and Emory University

May 2022

FRAMEWORK FOR A FIBRIN-SPECIFIC APTAMER FOR TARGETED DELIVERY OF FIBRINOLYTIC ESCHERICHIA COLI

Thesis committee:

Dr. Wilbur Lam
Biomedical Engineering
Georgia Institute of Technology

Dr. Valeria Milam
Materials Science and Engineering
Georgia Institute of Technology

Dr. MG Finn
Chemistry and Biochemistry
Georgia Institute of Technology

Dr. Anton Bryksin
Bioengineering and Biosciences
Georgia Institute of Technology

Date approved: May 2022

”Don’t ever tell me you can’t do something”

-*SAW*

This work is dedicated to my late father, Stephen Andrew White.

ACKNOWLEDGMENTS

I would like to thank the members of my thesis committee for their help and feedback during my time at Georgia Tech: Dr. Wilbur Lam for allowing me to work alongside his graduate students and providing biweekly feedback, Dr. M.G. Finn for great presentation feedback from him and his impressive lab group, and Dr. Valeria Milam for her advice and expertise in aptamer selection.

Additionally, I want to thank my colleagues. Jessica Lin for teaching me once unfamiliar laboratory techniques and providing great input and direction. You went above and beyond to provide the assistance I required and I am grateful for your leadership and support. Dr. Suneesh Karunakaran for his wisdom in solid-phase DNA synthesis. It was a pleasure to work alongside you on DNA synthesis. Molecular Evolution Core Laboratory's Naima Djeddar and Shweta Biliya for always lending a helping hand despite their busy schedules. Fang Shi, Adam Fallah, Nicole Diaz, Helya Taghian, Amina Alavarez, Dr. Samamntha Mascuch and the rest of the Molecular Evolution Core Lab members I have met during my time at Georgia Tech. You all have been great friends to me and you all have bright futures within the scientific community and beyond!

Lastly, I would like to sincerely thank Dr. Anton Bryksin for continuously providing me opportunities to advance my education. Your mentorship has provided a terrific graduate school experience and has adequately prepared me for a career in the biotechnology space. Your guidance is genuinely appreciated.

TABLE OF CONTENTS

LIST OF TABLES

LIST OF FIGURES

SUMMARY

Blood clots cause roughly 100,000 deaths each year making it an important health concern. Blood clots form as fibrinogen is polymerized by the enzyme thrombin, forming a fibrin clot structure. Current anticoagulant and fibrinolytic treatment approaches, including heparin and plasminogen activators, respectively, introduce the risk of bleeding when administered systemically due to the inability to differentiate a bad clot (causing heart attack or stroke) from a good clot (preventing bleeding). Engineered bacterial surface display of fibrinolytic proteins is an innovative synthetic biology approach to degrading fibrin while minimizing the bleeding risk, through enhanced release profiles and antibiotics, yet possess the issue of non-localized treatment. Here, methods to identify a fibrin-specific single stranded DNA (ssDNA) aptamer that exclusively binds to fibrin clots is proposed. Discovery of a fibrin-specific aptamer has many applications, including targeted delivery of engineered E. coli via biotin-streptavidin conjugation and as a biosensor for blood clot detection in laboratory or clinical settings. A fibrin clot, ssDNA library, Gibson assembly primers, dsDNA probes, dsDNA probe-mag bead conjugates, and dsDNA probe-cell conjugates were created as preliminary work. Utilization of these created products and continuation of the proposed methods provides the opportunity to identify a fibrin-specific aptamer for targeted delivery and biosensing applications.

CHAPTER 1
INTRODUCTION AND BACKGROUND

1.1 Nanotechnology in Cancer and Cardiovascular Disease

The traditional cancer treatments (chemotherapy, radiation, tumor-excision) and cardiovascular treatments (anti-thrombotic medication and surgery) have produced significant results in a variety of different scenarios for nearly a century. However, over the past few decades nanomedicine has revolutionized the therapeutic and diagnostic landscape in cancer (second leading cause of death) cardiovascular (leading cause of death) disease settings. Nanomedicine, defined as the use of nanoscale (1-100 nm) materials for diagnosis, delivery, sensing or actuation purposes in living organisms, offers many advantages over the traditional approaches [1]. Advantages nanomedicine approaches typically provide over the traditional treatments include increased drug efficacy, safety, sensitivity, and personalization to respective patients. These perks of nanomedicine have improved bioavailability, reduced toxicity, greater dose response, and enhanced solubility within the current therapeutic landscape [1]. The future of cancer and cardiovascular treatment will continue to become more specialized and patient-specific, with progress in nanotechnology permitting this advancement.

1.1.1 Nanotechnology in Cancer

Cancer nanotherapeutics have explored the ability to conjugate cytotoxic drugs, often encapsulated within a protective nanoparticle, to a polymer, antibody, or aptamer. The unique structural features of tumor vasculature permits enhanced permeability to nanomolecules, and the absence of an efficient lymphatic system allow greater retention of these nanomolecule conjugates [2]. This phenomenon, known as the enhanced permeability and retention effect

(EPR) effect [3], has allowed effective treatment of a multitude of otherwise inaccessible solid tumor types, including lung, breast, epidermoid, prostate and more. Additionally, the success in treatment of blood cancers has greatly improved since the introduction of nanotechnology approaches. For example, treatment of Non-Hodgkin's Lymphoma, the most common adult hematological cancer, took great steps with the introduction of Rituximab (Rituxan, Genentech/Biogen Idec). Rituximab is a chimeric monoclonal antibody targeted to B-cell antigen CD20 that enacts antibody-dependent cellular cytotoxicity (ADCC), complement-mediated cell death, and signaling apoptosis of malignant B cells. Randomized trial studies comparing different chemotherapy regimens showed greatly improved efficacy when Rituximab is included [4].

1.1.2 Synthetic Biology in Thrombosis

Deep Vein Thrombosis (DVT) and Pulmonary Embolism (PE) cause roughly 100,000 deaths each year making it an important health concern. The root issue is the formation of blood clots in response to artery or vein damage. Blood clots (or thrombus) form via the coagulation (or clotting) pathway when a blood vessel is damaged. A clot then impedes the bloodflow leading to a stroke (when blocking circulation to the brain) or a heart attack (when blocking circulation to the heart).

The key step of the coagulation pathway occurs when fibrinopeptides are cleaved by the serine protease thrombin, forming a fibrin clot structure [5]. Fibrinogen consists of two sets each of three different polypeptide chains: Aα, Bβ, and γ, crosslinked by 29 disulfide bridges. The six polypeptide chains are assembled with their N-term converged in a central "E" nodule, and the C-term of the Bβ and γ chains extend outward to from distal "D" nodules. The C-term of the A chains are globular and situated near the central E nodule of fibrinogen where they interact intramolecularly [6]. Once this step occurs, factor XIII can stabilize the formed fibrin clot by maximizing γ-chain cross-link stiffness [7].

A solidified clot can be degraded through anticoagulants and fibrinolytic agents. Cur-

rent anticoagulant and fibrinolytic treatment approaches, including heparin [8] and plasminogen activators [9], respectively, introduce the risk of bleeding when administered systemically. This arises due to the inability to differentiate a bad clot (causing heart attack or stroke) from a good clot (preventing bleeding). Engineered bacterial surface display of fibrinolytic proteins allow the ability to regulate anticoagulant activity through enhanced release profiles and antibiotics, improving the bleeding risk, yet still possess the issue of non-localized treatment. Here we propose using a newer nanotechnological approach to improve the targeted delivery of fibrinolytic E. coli.

1.1.3 Targeted Delivery

As discussed earlier, nanomedicine approaches exploit the physical, chemical, and biological properties of materials at the nanometer scale. Advancements in nanomedicine allow drug delivery to be achieved with maximum drug bioavailability and efficacy, controlled pharmacokinetics, pharmacodynamics, non-specific toxicity, immunogeneicity and biorecognition as well as the overcoming of obstacles arising from low drug solubility, degradation, fast clearance rates, relatively short-lasting biological activity and inability to cross biological barriers [10]. In particular, nanoparticles have become an increasingly popular mechanisms for carrying drugs and other biomolecules throughout the body. However, these nanoparticles often require assistance traveling to a specific location within the body. A novel strategy to achieve nanoparticle delivery to a specific target are Antibody Conjugated Nanoparticles (ACNPs). As the name suggests, ACNPs are nanoparticles with an antibody conjugated to the nanoparticle surface. Typically, the Fc region of the antibody will conjugate to the nanopartice via a polyethylene glycol (PEG) linker while the antibody binding domain stays exposed for target binding. This approach expands on antibody drug conjugates (ADCs) which were clinically evaluated in the late 1950s. To date, four ADCs have reached the market [11].

1.1.4 DNA and RNA Approaches in Biotechnology

In addition to proteins, like antibodies, DNA and RNA approaches have become increasingly popular within the biotechnology space since the advent of next generation sequencing (NGS). The genetic coding of proteins function of DNA and RNA has become a commonly exploited target for gene expression in cells . Different vector systems, like plasmid based vectors, allow for the transfer of genetic material into cells which ultimately upregulate or downregulated expression of a particular gene [12]. Additionally, the field of genetic engineering includes the manipulation of native (host) DNA through the three major genome editing technologies [13]: zinc-finger Nucleases (ZFN) [14], transcription-activator-like effector nuclease (TALEN) [15], and clustered regularly interspaced short palindromic repeat (CRISPR)-associated Cas9 nuclease [16]. Opposed to the other traditional coding roles DNA and RNA possess within cellular function, such as ribosomal RNA (rRNA) and transfer RNA (tRNA) within mRNA transcription and translation, a class of non-coding DNA and RNA segments (ncDNAs and ncRNAs) are being utilized for biotechnological applications. A variety of different small interfering RNA (siRNA; 21-23 nucleotide long dsRNA that inhibits expression of one specific target) [17], micro RNA (miRNA; 18-25 nucleotide long ssRNA that inhibits the expression of multiple mRNAs) [18], and antisense RNA (ssRNA that blocks the translation of a specific mRNA) [19] have been utilized in a multitude of cancer and cardiovascular strategies. These non-coding nucleic acids often repress gene expression by annealing to its complement mRNA within the the cell [20]. Study of DNA and RNA is also prominent within transcriptomics, the techniques to study the sum of all an organism's RNA transcripts [21], and metabolomics, the comprehensive examination of metabolites within biological systems [22], as downstream results of these practices often lead to further investigations of certain genes and gene regulators. As such, the ability to synthesize specific sequences efficiently has a large appeal.

1.1.5 Solid-Phase DNA and RNA Synthesis

In order to utilize DNA and RNA in the multitude of settings described above, oligonucleotides with the precise corresponding sequences must be created. To create these original DNA sequences, a quick, efficient, and inexpensive synthesis process is ideal. Solid-Phase DNA and RNA synthesis embodies this. Invented in the 1960s by Bruce Merrifield [23], solid-phase synthesis was such an important discovery Merrifield won the Nobel Prize for Chemistry in 1984. The main advantages this version of oligonucleotide synthesis has over solution synthesis include reduction of wasted reagents, no purification step needed each step, and the capability of automated synthesis via DNA or RNA synthesizers.

Solid-phase synthesis occurs in columns called controlled-pore glass (CPG) that enable all reagents and solvents to pass through freely. Different sized CPG pores are used to support oligonucleotides of different length. For example, 1000 angstrom CPG resin pores are capable of supporting oligonucleotides around 100 bases in length, but 2000 angstrom supports can be used longer oligonucleotides. In addition to the different pore sizes, using larger amounts of CPG support allows for higher concentrations of oligonucleotides to be synthesized (e.g. 3 mg of CPG supports 60 nanomole synthesis scale). The chemistry behind using these supports has undergone many iterations. The first methods of using a polymer support was developed by Mark Matteucci in 1980, where he discovered a method to cleave and isolate the resulting DNA from the polymer support with isolate high yield [24]. At this time protected and activated deoxynucleotide phosphites were used. The phosphites were then optimized, by Serge Beaucage, to protected 2'-deoxynucleoside 3'-phosphoramidites as synthons for the DNA synthesis [25]. These synthons proved to a crucial upgrade as they could be easily prepared, stored without decomposition, and create unprecedented internucleotide linkage yield upon activation with tetrazole [26]. These significant contributions by both Mark Matteucci and Serge Beaucage were achieved within the Marvin Caruther's laboratory at the University of Colorado Boulder.

Actual nucleotide addition proceeds in the 3'- to 5'- direction via a cyclical process

of linking phosphoramidites. The steps within the cycle include: (1) detritylation (where the DMT blocking group is removed with an acidic solution such as 3% dichloroacetic acid), (2) activation and coupling (where the nucleoside phosphoramidite in acetonitrile is activated by an acidic azole catalyst such as 5-ethylthio-1H-tetrazole), (3) capping (where free 5'-hydroxyl groups are protected from reacting in unintended coupling by a mixture of acetic anhydride and N-methylimidazole dissolved in tetrahydrofuran and pyridine), (4) oxidation (where the unstable phosphite-triester is converted to a stable tetracoordinated phosphate triester via iodine in tetrahydrofuran, pyridine, and water). These four steps are continued until the length of the desired oligonucleotide is synthesized. The final product is a protected ssDNA strand still attached to the CPG support.

In order to obtain the ssDNA oligonucleotide from the universal support and utilize the DNA for its intended purpose, the process of cleavage and deprotection (also called deblocking) must occur. Cleavage and deprotection happens via ester hydrolysis and dephosphorylation reactions. Ester hydrolysis can be achieved by ammonia treatment, while dephosphorylation requires treatment of a relatively strong base like methylamine. Since the last nucleotide of the ssDNA strand still possesses the blocking group, it must be removed via a deblocking procedure. Two options exist, standard or fast. The standard deprotection uses a water solution of ammonium and requires 12-15 hours at 45°Celsius or 6-8 hours at 60°Celsius. However, the fast deprotection method uses a water solution of both ammonium and methylamine mix (AMA). The time of this deprotection is 20 minutes with temperature of 45°Celsius or 2-3 hours at 20°Celsius. The fast deprotection is reserved for the deprotection of standerd and a few modified oligonucleotides. Oligonucleotides that include special phosphoramidites, including fluorophores or chemical phosphorylation reagent, require the longer, standard deprotection method or possess a unique recommended method provided by the reagent supplier.

Finally, once the oligonucleotide is removed from the CPG support and the DMT group of the final oligonucleotide is removed, the DNA must be dried. This can be accomplished

with a vacuum centrifuge (or vacufuge). The vacuum centrifuge, first used to isolate viral DNA in 1936 by Johannes Bauer [27], facilitates fast, efficient, and gentle vacuum concentration of DNA, RNA, nucleotides, proteins and other liquid samples. As its name implies, it works by creating a sediment layer of the DNA product via centripetal forces and removing the aqueous layer via a vacuum. The final product of using a vacufuge is the dried DNA oligonucleotide

Table 1.1: List of steps and corresponding reagents involved within solid-phase oligosynthesis.

Reagent List	
Step	**Reagent**
De-blocking (detritylation)	3% trichloroacetic acid (TCA) in dichloroethane (DCE)
Activation and Coupling	0.25M 5-ethylthio-1H-tetrazole and 0.1M dA, Ac-dC, dmf-dG, dT, or Chemical Phosphorylation Reagent II in acetonitrile
Capping	15% acetic anhydride in tetrahydrofuran (Capping Mix A) and 16% 1-N-methylimidazole in tetrahydrofuran (Capping Mix B)
Oxidation	0.02M Iodine in Tetrahydrofuran/ Pyridine/ Water (88:10:2)
Cleavage and Deprotection	40% Methylamine in Water or Ammonium Hydroxide and Methylamine (1:1 v/v)

1.2 Aptamers

It has been 155 years since Gregor Mendel published his work on the heredity of peas. Since then, DNA has been studied extensively and found to have various purposes. However, three key events have proven pivotal to the advancement of DNA practices. These include Sanger Sequencing in 1977 [28], Polymerase Chain Reaction (PCR) in 1983 [29], and development of oligosynthesis techniques in the 1980s [23]. The ability to synthesize a tremendous number of different oligonucleotides, create many copies of these sequences, and determine the exact sequence of a particular oligonucleotide has allowed current genetic engineering feats, including the invention of target-specific aptamers.

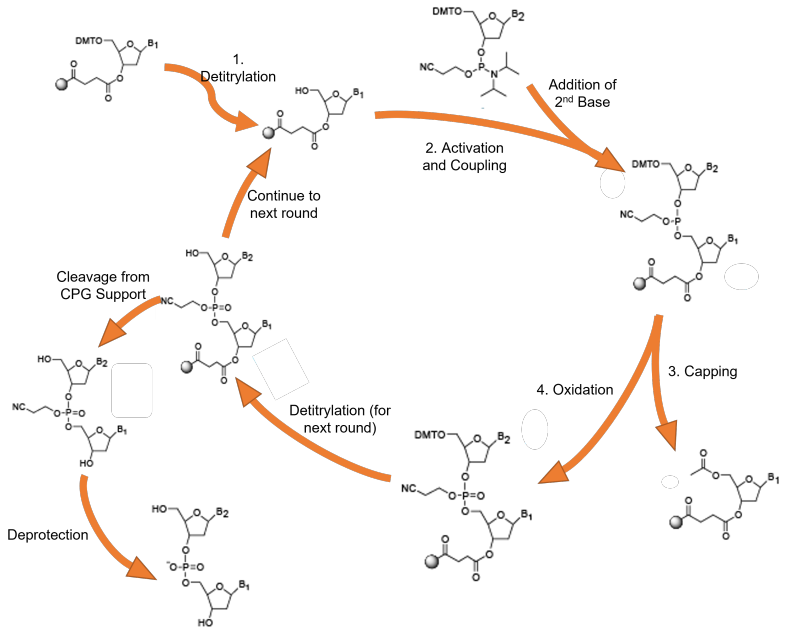

Figure 1.1: Solid-phase oligonucleotide synthesis cycle. Shown are the intermediate products of the detitrylation, activation and coupling, capping, oxidation, cleavage, and deprotection steps. Modified from ATDBio Nucleic Acids Book by Tom Brown.

1.2.1 Aptamer History

In 1990, then PhD student Craig Tuerk was studying the translational regulation of the DNA polymerase gene of the bacteriophage T4. When recognizing the negative feedback loop when polymerase concentration reached high levels, Tuerk studied the sequence/structure that overlapped the ribosome binding site. A hairpin with an intramolecular loop of eight nucleotides was identified. Dr. Craig Tuerk then synthesized every possible loop sequence (all 4^8 of them) and studied binding to the polymerase. Two sequences emerged, and Tuerk and his then advisor Larry Gold began thinking of RNA as "shapes, not tapes" [30]. Thus, aptamers are defined as single stranded DNA or RNA oligonucleotides that fold into 3D structures and bind to non-nucleic target with high specificity. Since Tuerk's discovery, a multitude of aptamers forming different conformations have been identified. Like proteins, aptamers fold into different conformations based on different intramolecular interactions. Intramolecular interactions follow the same base pair rules (Guanine binds to Cytosine Adenine binds to Thymine (or Uracil if RNA)) seen in dsDNA.

Aptamer Library

In order to perform SELEX, one must possess a library of various ssDNA segments. Aptamers obtain their variability through their unique ssDNA sequence. The general structure of an aptamer library has 3 regions: a variability region and 2 constant regions that flank the variability region. The variability region will cause different folding much like different amino acid sequences causes different protein folding. The number of possible sequences is: number of possible sequences = 4^n where 4 represents the four possible nucleotides (adenine, cytosine, guanine, and thymine) and n represents the number of nucleotides within the variable region. However, recent literature has shown four consecutive guanine nucleotides can create a G-quadruplex structure which could hinder folding variability and, thus, target-specificity [31]. To prevent a G-quadruplex from forming, all nucleotides except guanine can be added to every fourth nucleotide, which makes the total number of possible sequences: number of possible sequences = $4^{3n/4} * 3^{n/4}$.

In my work, I synthesized a ssDNA library with the two constant regions (20 nucleotides and 22 nucleotides) on the ends and a 40 nucleotide long variable region in the middle of the oligonucleotide. The variable region utilized the strategy to avoid a G-quadruplex formation by having a general structure of 'NNNH' repeated 10 times, where N represents any nucleotide and H represents any nucleotide except Guanine.

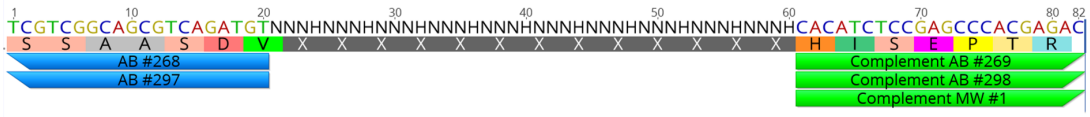

Figure 1.2: ssDNA aptamer library design with (NNNH)x10 variable region to minimize G-quadruplex formation. Forward primers AB 268 and AB 297 (5'- biotin tagged) can be used to amplify or functionalize the selected sequences, respectively. Reverse Primers AB 269, AB 298 (5'- Cy5 tagged), and MW 1 (5'- phosphorylation tagged) can be used for PCR amplification, dsDNA probe tracking, and antisense strand degradation, respectively.

1.2.2 Systematic Evolution of Ligands by Exponential enrichment (SELEX)

The process by which aptamers are discovered is called Systematic Evolution of Ligands by Exponential enrichment (SELEX) [32]. SELEX is a cyclical process that is repeated until a select group of high-affinity aptamer candidates are remaining. The steps within the cycle include aptamer folding (where the aptamer library is denatured at high temperatures then snap cooled to ensure proper folding conformation), incubation of folded aptamer candidate library with the target molecule (where the properly folded aptamer candidates are given time to bind to a desired target), washing of unbound or low-affinity sequences (where the aptamers not specific for the desired target are eliminated from the library), elution of positively selected nucleotides (where the aptamers with moderate to high affinity for the desired target remain in the library for successive rounds), PCR amplification (where the moderate to high affinity aptamers are amplified to a high enough concentration needed for the next round of SELEX), and pool conditioning (where the antisense strand of the ds-DNA PCR product is digested by an enzyme, like Lambda Exonuclease [33], so the ssDNA library is ready for the next round of SELEX). Typically, SELEX is 10-15 rounds with the first round lasting 10-12 hours, and successive rounds lasting 4-6 hours. Aptamer progress is monitored throughout the selection process, mainly via gel electrophoresis. When the aptamer library is no longer decreasing, the remaining aptamers can be sequenced. Given multiple aptamers may be specific towards the desired target, next generation sequencing (NGS) must be performed. A forward primer with an NGS adapter can amplify the remaining sequences while also making the sequences compatible to the MySeq or ISeq flow lawn . Once the final target-specific aptamer sequences are identified, the binding kinetics of the selected aptamers can be characterized through binding affinity assays.

1.2.3 Competition-Enhanced Ligand Selection (CompELS)

In 2018, Dr.Valeria Milam at Georgia Institute of Technology developed a different methodology to identify DNA aptamers. This method, named competition-enhanced ligand screen-

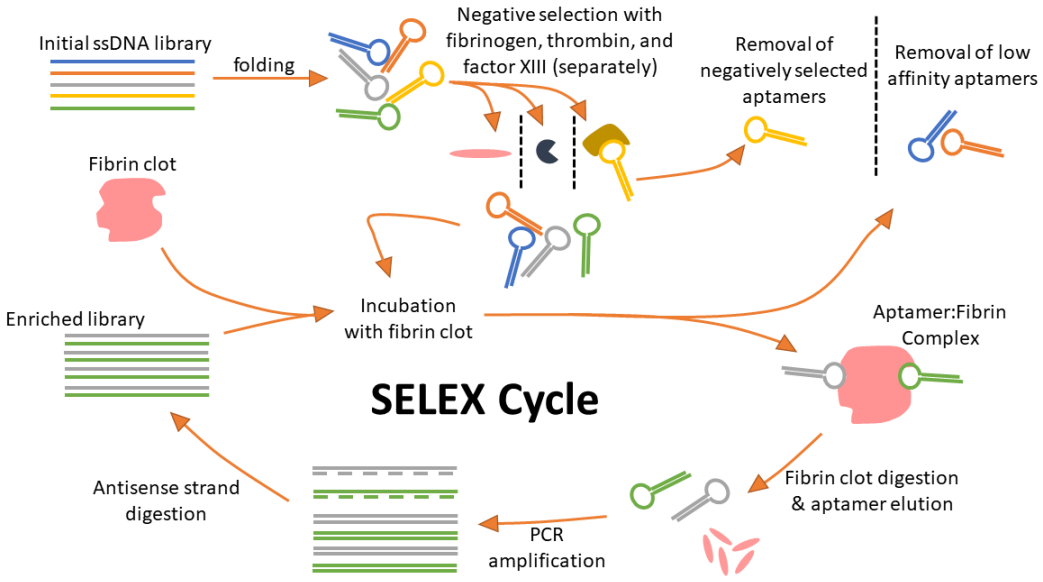

Figure 1.3: SELEX cycle to identify a fibrin-specific aptamer. Negative selection is performed by incubating the library with each fibrinogen, thrombin, and factor XIII prior the beginning the SELEX cycle. Sequencing and characterization of the final fibrin-specific aptamers is performed after 10 rounds of SELEX or when no visible decrease is seen between two successive rounds of removed low affinity aptamers.

ing (CompELS), differs from SELEX in that the iterative elution and PCR amplification step is omitted [34]. CompELS offers a few advantages to aptamer discovery including reducing complexity, saving time, and lowering costs per each round of aptamer screening. The concept of reducing the complexity and time of aptamer screening has been a focus since the in vitro process began in 1990. A notable SELEX variant is RAPID-SELEX (RNA Aptamer Isolation via Dual-cycles SELEX). This process systematically skips unnecessary amplification while still maintaining the ability to identify quality target-specific aptamers [35]. CompELS takes this feature a bit further by removing the systematic, alternation of PCR and PCR-free rounds and is completely PCR-free. The main advantage of a completely PCR-free approach, regarding to the selection process of a high-quality aptamer, is the ability to introduce a variety of unenriched random sequence populations [36]. As mentioned earlier, an aptamer library possess a variable region flanked by two constant regions. During SELEX, a researcher will begin the selection process with only

one library then amplify the eluted sequences within that library. Within CompELS, however, a multitude of libraries of various variable region design and length can be introduced to the target assay simultaneously or subsequently. Given the 'black-box' nature of aptamer selection, meaning the final aptamer sequence is extremely unpredictable, selecting an optimal library for a particular target is ambiguous. The utilization of multiple libraries during CompELS minimizes this ambiguity and increases the probability of highest-affinity aptamer discovery.

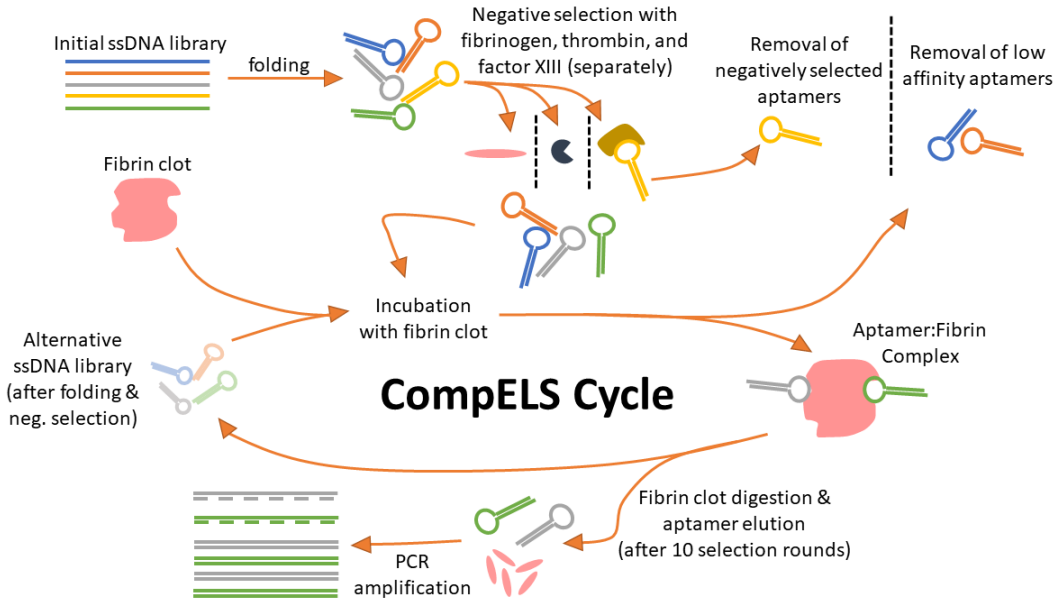

Figure 1.4: CompELS cycle to identify a fibrin-specific aptamer. CompELS differs in SELEX as it only has clot digestion, aptamer elution, and PCR amplification after the final round of CompELS screening in preparation for sequencing, cloning, and characterization purposes. Various different libraries may be used during different rounds of CompELS.

1.2.4 Aptamer Applications

As mentioned earlier, a large number of aptamers have been discovered since the capability of ssDNA to fold and bind to targets was founded in 1990. Given the fast and relatively simple in vitro process of SELEX and CompELS, the number of novel aptamers specific to a wide range of targets continue to grow rapidly. It did not take long for scientists to

develop creative ideas to implement aptamers to biotechnological applications. The list of aptamer applications include use in drug delivery, environmental monitoring, clinical diagnostic, molecular biosensor, target capture, biomarker discovery, bioimaging, in vivo therapeutics, selective chromatography, and more [37].

The most interesting of these applications is the use of ssDNA as an in vivo therapeutic. Currently, there are 9 aptamers used as therapeutics: Pegaptanib (inhibits the interaction of VEGF with VEGFR1/2 for treatment of age-related macular degeneration (AMD)), AS1411 (binds to cell-surface nucleolin then cytoplasmic nucleolin to prevent cancer cell proliferation), REG1 (factor IXa-specific antithombotic that prolongs clotting times in activated partial thromboplastin time assays), ARC1779 (antithrombotic that binds to A1 domain of von Willebrand factor to inhibit binding to platelet membrane glycoprotein Ib rececptor), NU172 (antithrombotic that binds and inhibits at exosite 1), ARC1905 (binds to complement component 5 (C5) which plays a role in AMD), E10030 (binds to platelet-derived growth factor (PDGF)), NOX-A12 (binds to chemokine ligand 12 (CXCL12) to inhibit affect the homing, mobilization and retention of autologous hematopoietic stem cell transplants), and NOX-E36 (binds to chemokine ligand 2 for treatment of type 2 diabetes) [38]. Of these 9 different aptamers, only Pegaptanib is FDA approved. The role of aptamers as a therapeutic agent is typically antagonistic as they act as competitive inhibitors. They are able to block protein-protein interactions like receptor-ligand interactions, however downstream phosphorylation is not possible as seen with antibodies (as discussed in the Aptamers vs. Antibodies section).

Aside from therapeutics, another relevant application, with regards to this work, include aptamers as biosensors. Since primers can be modified on the 3' and 5' end, a large quantity of functionalized aptamers can be created via PCR for a variety of purposes. In our context, a fluorescent dye, such as Cy5, added to the 5'- end of the fibrin-specific aptamer will create a novel fibrin biosensor. Upon intravascular injection of the 5'- fluorescently labelled fibrin-specific aptamer, the nanoscale sized biomolecule can infiltrate and bind to the

porous fibrin clot wherever present within the circulatory system. The fluorescent tag can then be monitored via in vivo fluorescent imaging techniques. Near-infrared fluorescent in vivo imaging has become increasingly popular and shown good imaging results within mice [39]. Plus, the increased use of DNA/RNA probes (DNA/RNA with a fluorophore that complement a particular sample DNA/RNA fragment) for genomics, transcriptomics, and qPCR applications has increased the need for fluorescent amidites. As such, a large repertoire of fluorescent amidites [40] and CPG supports have been created.

In addition to biosensors, a fibrin-specific aptamer can be functionalized as a targeted delivery device. A prominent way aptamers are used as a targeted delivery device is by the formation of aptamer-drug conjugates. Aptamer-drug conjugates, where a ssDNA oligonucleotide able to bind to a desired target is conjugated to cytotoxic drugs, can deliver potent material to a cell. In the context of cancer, conjugation of monomethyl auristatin E (MMAE) and monomethyl auristatin F (MMAF) to an aptamer targeting prostate cancer cell lines has shown to successfully reduce the tumor volume and prolong the lives of mice with prostate cancer [41]. Another way aptamers can serve as targeted delivery agents is by aptamer-nanoparticle or aptamer-cell conjugation. As mentioned earlier, nanoparticles and synthetic biology practices have advanced to address a multitude of issues. Nanoparticles and cells are both capable of expressing a variety of proteins on their surface, allowing them to conjugate to other biomolecules through protein:protein interaction. One of the most frequently exploited protein:protein interactions used in molecular biology is the streptavidin:biotin interaction [42]. Given the strong binding affinity between streptavidin and biotin [43] and the ability synthesize 5'- biotinylated oligonucleotides [44], there is a large appeal to develop cells able to display streptavidin on the cell surface. During my time at Georgia Tech, I have aimed to progress the function and use of aptamers from an aptamer-drug conjugate to an aptamer-nanoparticle or aptamer-cell conjugate, comparable to the progression of ADCs to ACNPs (mentioned in the Nanotechnology in Cancer section).

1.2.5 Aptamers vs. Antibodies

Aptamers not only offer many benefits in terms of ease and efficiency, but also are highly advantageous in terms of production and logistical costs. Currently, the cost of goods per gram for monoclonal antibodies (mAb) produced in mammalian systems ranges from $260 to $1500 [45]. Aptamers, however, have a more favorable cost of goods per gram ranging from $300/gram for small-scale (¡ 1 g) volumes to $50 per gram for large-scale (¿1 g) volumes [46]. Differences in the means of production account for a large portion of the price differences seen. Monoclonal antibodies require greater capital investment, being produced in animal systems (in vivo) as opposed to chemically (in vitro) like aptamers. On a laboratory scale, conservative cost estimates for monoclonal antibody development and production are around $8600 . Conversely, Chimerx and Roboklon have developed kits for highly optimized versions of the SELEX workflow ranging from $245 to $320. The cost of initial nucleotide libraries and PCR is exceptionally low, especially when compared to the cost of immunizing mice. These prices for aptamers also have high potential for further reduction with optimization of the selection processes and logistical advantages. Companies have been working for decades to optimize and streamline the production of monoclonal antibodies (especially through cellular culture studies). Similarly, aptamers will only increase in cost effectiveness once they undergo the same push for SELEX process optimization. On the level of large-scale production, aptamers already hold several advantages over antibodies as well. Aptamers have a molecular weight ranging from 12-30 kDa, which is much smaller than the average 150–170 kDa for antibodies. This characteristic allows the same volume of produced goods to have a higher number of functional molecules, giving aptamers higher cost effectiveness relative to monoclonal antibodies. Aptamers smaller size also allows increased access to tissues, potentially making the same volumes more effective [46]. Hybridomas, on the other hand, have several factors increasing logistical costs. Hybridomas, which are B lymphocytes somatially fused with myeloma cells, typically require cryo-preservation for long term storage. In addition to the improper storage

risk, hybridomas have the potential for genetic instability and failure to produce antibodies over time [47]. Aptamers, being chemically synthesized, are highly reproducible so only the sequence information needs to be stored to be recreated later. Oligonucleotides are also able to endure many thaw cycles. The higher stability of aptamers allows them to persist at ambient temperatures, giving them a much longer shelf life and cheaper transportation costs relative to hybridoma cells [48]. These differences in reproducibility, stability and storage make aptamers more reliable for large-scale production and reduce several logistical costs for an already more cost-effective process.

Table 1.2: Table comparing the pros and cons of aptamers and antibodies.

Aptamers vs. Antibodies		
Criteria	Aptamers	Antibodies
Material	Nucleic Acid	Amino Acids
Binding Type	Surface Recognition	Binding Pocket (Lock and Key)
Binding Affinity	High (kD: μM - nM)	Very High (kD: nM-pM)
Discovery Method (Time)	In vitro SELEX and CompELS (2-5 weeks)	Hybridoma ($\geq$ 6 months)
Cost	Low	Variable
Stability	Long shelf-life with reversible denaturation	Limited shelf-life with irreversible denaturation
Size	Very Small (12-30 kDa)	Small-Medium (150-170 kDa)

1.2.6 Aptamer Limitations and Solutions

The most prominent issues with aptamers, and likely why they are not as widely used as antibodies, are due to susceptibility to degradation and rapid excretion from the bloodstream. DNA is typically within the nucleus of a cell, meaning there is a cell membrane and a nu-

clear membrane to protect the nucleic acids. However, when the ssDNA is introduced in the bloodstream, free nucleases and pores within the blood vessels can quickly digest or filter the small DNA molecules, respectively. Because of these two in vivo issues, aptamers that are not equipped to face degradation and filtration can possess a half life less than two minutes [38].

Modified nucleotides are used to address the issue of nuclease degradation. There are a multitude of options when it comes to modifying nucleic acids. Researchers have examined the impact of modifying either the sugar-phosphate backbone or modifying the heterocyclic bases. A particularly vulnerable site of nuclease activity is the 2'- position of deoxyribose residues [49]. The first nucleotide derivatives with alterations at the 2'- position of (deoxy)ribose was a 2'-aminopyrimidine RNA aptamer targeting human neutrophil elastase [50]. While aptamer stability increased with this modification, issues with synthesis and proper aptamer folding developed. An alternative to 2'-aminopyrimidine substitutions is a 2'-F-deoxyribopyrimidine modification. This modification showed similar stability while also possessing a higher binding affinity to its respective target then the 2'-aminopyrimidine ligands [51]. In fact, the RNA aptamer targeting VEGF that served as a template for pegaptanib, the first and only FDA approved aptamer used for treatment of age-related macular degeneration (mentioned earlier), utilizes both 2'-F-pyrimidine and 2'-methoxy-purines to increase nuclease resistance [52].

With regards to renal filtration, the endothelium of blood vessels has relatively large pores of 70-100 nanometers in diameter. Thus, small molecules below roughly 50 kilodaltons, which include aptamers (5-15 kDa see Table 1.2, are subject to excretion from the bloodstream. In order to prevent renal filtration, aptamers are commonly conjugated to a high molecular mass poly-ethylene glycol (PEG) linker. A 20 kDa and 40 kDa PEG conjugated aptamer was compared to its non-conjugated version. The 40 kDa PEG conjugated aptamer sustained the highest concentration within the bloodstream after 1 day of monitoring, followed by the 20 kDa PEG conjugated aptamer, then the non-conjugated aptamer

[38].

1.3 E. coli Surface Display

E. coli is considered the model bacterium due to its presence in the human microbiota and comprehensive genome knowledge. Being a gram-negative bacteria with an inner and outer membrane, proteins are restricted from releasing from the cell. Special systems exist to transport extracellular proteins to the surface. These proteins are able to remain anchored to the cell surface or be cleaved off and released to the surrounding environment via membrane blebbing (or membrane vesicle formation). Display for practical synthetic biology applications: including live vaccine development, display of antibody and peptide libraries, production of whole cell adsorbents, expression of catalytic activity, and more [53] [54]. Designing plasmids that utilize these systems allow desired gene products to be incorporated and displayed on the cell surface of parent and daughter cells. Our previous attempts using PET autotransporter and monovalent streptavidin showed inconsistent results. Thus, we investigated using different surface display systems and streptavidin genes to provide sufficient streptavidin expression for biotinylated aptamer conjugation. A total of three different surface display systems and three different streptavidin genes were used to construct nine different vectors. The presence and quantity of streptavidin expressed can be quantified via the use of a dsDNA probe where the sense strand possesses a 5' biotin tag and the antisense strand has a 5' fluorescent tag. After incubation of the dsDNA probe with the streptavidin expressing E. coli cells, flow cytometry can be performed to assess which surface display system and which streptavidin gene provides optimal expression.

1.3.1 Lpp-OmpA

The Lpp-OmpA-mediated surface display has opened tremendous possibilities in the synthetic biology realm: including autofluorescence [55], streptavidin-biotin conjugation [56] [57] [58], proteins including β-lactamase [59], protein E [57], methyl parathion hydrolase

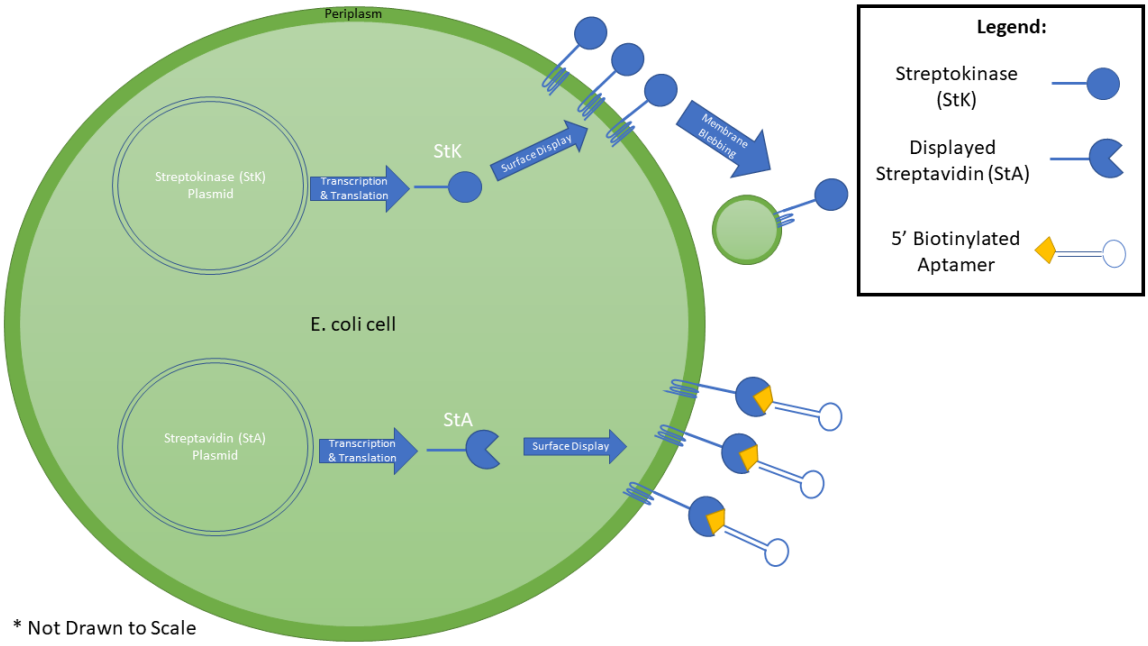

Figure 1.5: Schematic of surface display streptokinase (StK) and streptavidin (StA). Proteins are displayed by different surface display systems and are either expressed on the E. coli cell surface or released into the surrounding tissue via membrane blebbing.

(MPH) and enhanced green fluorescent protein (EGFP) fusions, and more. It consists of the major lipoprotein (Lpp) and OmpA proteins. The Lpp serves as signal peptide domain that targets and anchors the tribrid to the outer membrane, while the OmpA is an outer membrane protein required for surface expression of the passenger protein due to its transmembrane domain consisting of an eight-stranded β barrel [53].

1.3.2 pAIDA1

Adhesin involved in diffuse adherence (AIDA) is another popular autodisplay technology used with E. coli. This autodisplay system has been reported to express approximately 1.6×10^5 streptavidin molecules on the outer membrane of a single E. coli cell [60], making it a viable surface display system for synthetic biology applications.

1.3.3 Streptavidin Plasmid Constuct

As mentioned earlier, the streptavidin-biotin conjugation has become an exploited protein:protein interaction within the bionanotechnology world. A varitey of streptavidin variants have been created to increase its binding affinity and number of binding sites for biotin. The most utilized streptavidin is the tetravalent version that has four subunits with the same initial binding affinity for biotin. However, examination of the streptavidin:biotin interaction via atomic force microscopy (AFM)-based single-molecule force spectroscopy (SMFS) showed binding geometry and conformational changes impact the the streptavidin binding pocket and, thus, the binding affinity [61]. The phenomenon of how binding affinity of other binding pockets is influenced positively or negatively upon prior ligand binding to other binding sites is known as cooperativity [62]. Several streptavidin gene designs have been incorported as a passenger protein within the Lpp-OmpA and pAIDA1 surface display systems. A single-chain tetravalent [63], multiple subunit tetrameric [60], dual chain pseudotetrameric [64] [65], homotetrameric [56], and other tetravalent streptavidin designs have been shown to properly display on the surface of E. coli cells. While divalent [66] and monovalent [67] streptavidin variations have been successfully created, optimal biotinylated aptamer binding is expected to occur when conjugating to the multiple binding sites of a tetravalent streptavidin as more biotin molecules can coat the surface.

1.4 Conjugating Fibrinolytic E. coli with a Fibrin-Specific Aptamer

The scope of this work is to provide a targeted delivery strategy for fibrinolytic E. coli cells designed by Jessica Lin. These cells obtain the fibrinolytic feature by surface display and release of streptokinase, a known plasminogen activator [68]. To address the issue of non-localized treatment, the E. coli cells were designed to co-express streptokinase with streptavidin. Streptavidin expression on the E. coli cell surface allows the tethering of a 5'-biotinylated fibrin-specific aptamer to the bacteria cells and aggregation of cells to the

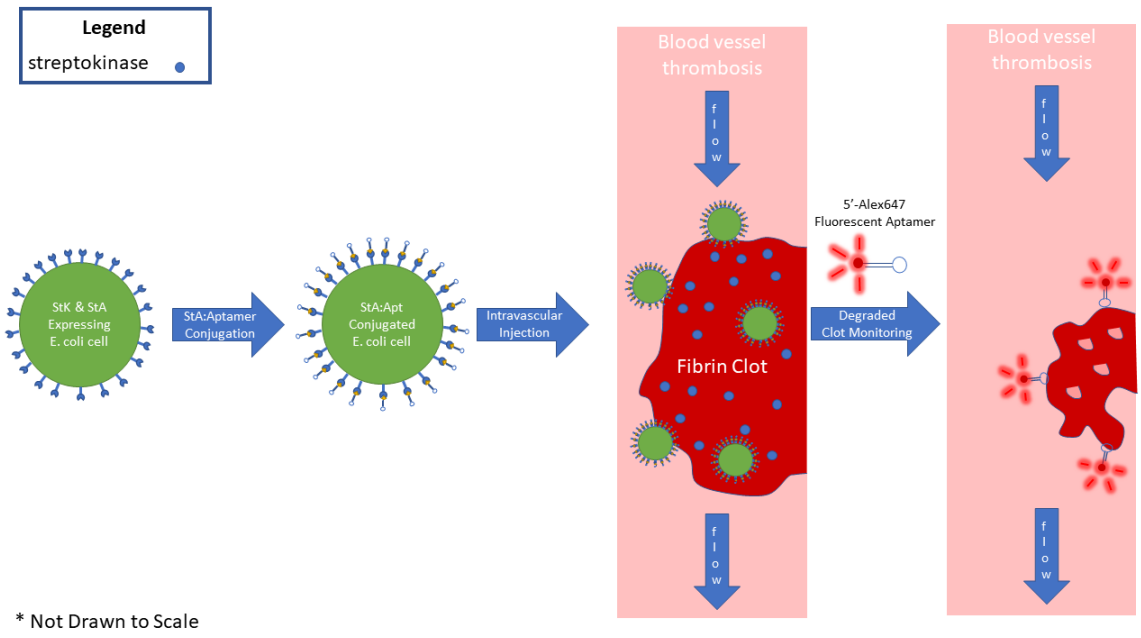

Figure 1.6: Schematic of using a fibrin-specific aptamer as a targeted delivery and biosensor agent. 5'-biotinylated fibrin-specific aptamer is conjugated to streptavidin (StA) and streptokinase (StK) expressing E. coli. Cells are introduced to the blood stream via intravascular injection, localized to the fibrin clot via aptamer binding, degradate the clot upon streptokinase release, then removed from the blood stream with antibiotic treatment. 5'-fluorescently labelled aptamer shown as a fibrin biosensor within clot monitoring context.

fibrin-clot area. Additionally, as mentioned earlier, the fibrin-specific aptamer can be purposed as a clot monitoring biosensor (see Figure 1.6). This work provides the framework for discovering a fibrin-specific aptamer and how to functionalize the aptamer for in vivo use.

CHAPTER 2

METHODOLOGY

2.1 Fibrin-Specific Aptamer

2.1.1 Fibrin Clot Formation

In order to discover the optimal fibrin clot, an array of 6 different 10 mg/mL fibrinogen and 1 kU/mL thrombin amounts were incubated and analyzed (see Table 2.1. 100 μL or 200 μL of fibrinogen and 1 μL, 2 μL, or 3 μL of 1 kU/mL thrombin was incubated with 2 μL mg/uL factor XIII and 2 μL of $CaCl_2$ for 30 minutes at 37°.

Table 2.1: Array of 6 different fibrinogen and thrombin combinations for fibrin clot formation within 2 mL eppendorf tubes. 100 μL or 200 μL of fibrinogen and 1 μL, 2 μL, or 3 μL of 1 kU/mL thrombin was incubated with 2 μL mg/uL factor XIII and 2 μL of $CaCl_2$.

Fibrin Clot Formation		**Fibrinogen (10 mg/mL)**	
		100 uL (1 mg)	200 uL (2 mg)
Thrombin (1 kU/mL)	1 uL (1 U)	1	4
	2 uL (2 U)	2	5
	3 uL (3 U)	3	6

2.1.2 Oligonucleotide Synthesis

The 82 nucleotide long library design (5'-TCGTCGGCAGCGTCAGATGTNNNHNNNHNNNHNNNHNNNHNNNHNNNHNNNHNNNHNNNHCACATCTCCGAGCCCACGAGAC), 22 nucleotide long phosphorylated and non-phosphorylated reverse primer (MW #1: 5'-(P)GTCTCGTGGGCTCGGAGATGTG) (see Figure 1.2), and 85 nucleotide long probe template (5'-TCGTCGGCAGCGTCAGATGTGTATAAGAGACAGTCHNWCTCCACCAHNWCGCTGTCTCTTATACACATCTCCGAGCCCACGAGAC) (see Figure 2.1c.) were synthesized using the ASM-2000 DNA/RNA Synthesizer here at the Georgia Tech Molecular Evolution Core Lab. Additionally, 27 different primers used for

Gibson assembly of the streptavidin surface display plasmid construction were synthesized (see Table 2.3).

Synthesis Plate Preparation

1000ÅUniversal UniLinker Support (ChemGenes, Wilmington, MA, Cat. #N-4000-10, Lot #KP23-42) was suspended in 57% dibromomethane (Thermo Fisher Scientific, Ward Hill, MA, Cat. #A10456, Lot #10215970) and 43% chloroform (VWR, Radnor, PA, Cat. BDH83626.400, Lot
18090405) to form a 10 mg/mL CPG suspension. 300 μL of 10 mg/mL CPG suspension was loaded onto a synthesis plate to support a 60 nanomole synthesis scale. Vacuum was applied to remove liquid from wells and pack CPG on the well filter. The CPG support was washed once with 500 μL of acetonitrile (Honeywell Burdick Jackson, Muskegon, MI, Cat. #LC015-1, Lot #DP339) then liquid was removed from the wells by vacuum. A 3 mm puncher was used to create a glass wool filter to place in the wells on the CPG support.

Deblocking

300 μL of 3% trichloroacetic acid (TCA) in dichloroethane (DCE) (Sigma-Aldrich, St. Louis, MO, Cat. #284505-1L, Lot #SHBL8292) was added to each well and incubated for 9 seconds before liquid was removed via vacuum. As a quality control, the 5'- dimethoxytityl (DMT) group was collected during the first and last steps of the oligosynthesis cycle for non-phosphorylated oligos and first, last, and second-to-last steps for phosphorylated oligonucleotides. Color absorbance of DMT group was monitored both visually and by BioTek Syngergy H4 plate reader. A washing step of 520 μL of low water content acetonitrile (VWR, Radnor, PA, Cat. #BDH1105-4LG, Lot #0000248575).

Coupling

dA (Cat. #10-1000-SP, Lot #G005430-5), Ac-dC (Cat. #10-1015-SP, Lot #G004477-14), dmf-dG (Cat. #10-1029-SP, Lot #G005431-2), dT (Cat. #10-1030-SP, Lot #G004503-10), and Chemical Phosphorylation Reagent (Cat. #10-1901-02, Lot #G109431) from GlenResearch (Sterling, VA) were diluted in acetonitrile to a 0.1M concentration then installed in the ASM-2000 DNA/RNA synthesizer. 210 μL of 0.1M dA, Ac-dC, dmf-dG, or dT and 210 μL of activator solution, 0.5M 5-Ethylthio-1H-Tetrazole in Anhydrous Acetonitrile (GlenResearch, Sterling, VA, Cat. #30-3240-71, Lot #G905720), was added to the wells and incubated for a coupling time of 35 seconds except during the first nucleotide addition. During the first nucleotide addition, 170 μL of the DNA amidites were added with an incubation coupling time of 35 seconds. Chemical Phosphorylation Reagent, added on the 5'-end during the last cycle of the synthesis (since solid-phase synthesis occurs in the 3'- to 5'- direction), had an incubation time of 6 minutes as instructed by GlenResearch. Vacuum is applied after the incubation period to remove the remaining amidites or chemical phosphorylation reagent liquid from the wells then 400 μL of acetonitrile is dispensed to wash the wells briefly (4 seconds) before vacuum is applied.

Capping

200 μL of capping mix A, Tetrahydrofuran/ Pyridine/ Acetic Anhydride (GlenResearch, Sterling, VA, Cat. #40-4110-62, Lot #G003730), and 200 μL of capping mix B, 16% methylimidazole in tetrahydrofuran (GlenResearch, Sterling, VA, Cat. #40-4220-62, G002740) are added to the wells simultaneously and incubated for 18 seconds except during capping of the first nucleotide addition. 170 μL of capping mix A and B are added and incubated for 18 seconds during capping of the first nucleotide addition. Vacuum is applied to remove the remaining capping mix A and B, then wells are washed with 500 μL of acetonitrile. Acetonitrile is incubated for 4 seconds before vacuum removes washing liquied from the wells.

Oxidation

270 μL of 0.02M iodine in tetrahydrofuran/ pyridine/ water mix in an 88:10:2 ratio, respectively, is added to each well and incubated for 21 seconds before the oxidation reagent liquid is removed via vacuum. Wells were then washed with 600 μL of acetonitrile.

Cleavage and Deprotection

Two different methods were used for oligonucleotides with and without 5'- phosphate group tags. The fast deprotection method, mentioned earlier in the introduction, was utilized for standard oligonucleotides without the 5'= phosphate group. The fast deprotection method consisted of four additions of 100 μL 40% methylamine in water (Sigma-Aldrich, St. Louis, MO, Cat. #426466, Lot #SHBK3657) with vacuum of liquid into collection tubes (400 μL total volume of ssDNA in methylamine solution). Each treatment of methylamine was left to incubate in the wells for 10 minutes before vacuuming into collection tubes. The tubes of eluted ssDNA solution was then placed within the deprotection tool and incubated at 45°for 1 hour. Cleavage and deprotection of oligonucleotides with the 5'-phosphate modification consisted of 4 treatments of 150 μliter (15 minute incubation time for each treatment) of ammonium hydroxide and methylamine mix (1:1 v/v) then incubated at 65°C for 30 minutes.

Drying and Resuspension

After deprotection has occurred, drying of the ssDNA oligonucleotide must occur. The product volume was transferred to a 2 mL eppendorf tube then sealed with parafilm with 5 holes punched with a needle. Eppendorf tubes were run on a vacufuge for 10 hours at 30°C to permit sufficient drying. Eppendorf tubes with dried oligonucleotides were collected then resuspended in 50 μL of 10 mM Tris HCl with 50% glycerol. ssDNA concentration was measured via nanodrop spectrophotometer. The ssDNA oligonucleotides were then diluted and stored at 100 μM.

2.1.3 SELEX

Systematic Evolution of Ligands by Exponential enrichment (SELEX) includes the following cycle steps: aptamer folding, target incubation, separation of unbound aptamers, elution and amplification of bound aptamer, and antisense strand digestion of dsDNA PCR product. After the bound aptamers are eluted each round, 3% gel electrophoresis is performed @ 90 Volts for roughly 50 minutes to monitor the thickness of the DNA bands. Once the band thickness is no longer thinning, no more rounds of SELEX need to be performed and aptamer identification can be performed. Prior to beginning the selection process, negative selection was performed to remove any aptamers that possess affinity for fibrinogen, thrombin, factor XIII, or the binding buffer (20 mM Tris/HCl (pH 8.0), 150 mM NaCl, 5 mM KCl, 1 mM $MgCl_2$, 0.1% Tween 20).

Aptamer Folding

The 100 μM aptamer library in binding buffer was removed from -20°C storage. The library was then denautred at 95°C for 5 minutes then snap-cooled on ice until ready for use.

Negative Selection

Prior to beginning the selection process, negative selection was performed via subsequent addition of the folded library to coated wells of fibrinogen, thrombin, factor XIII, and binding buffer. Once the library was removed from the final well, the negatively selected aptamers were resuspended in binding buffer and monitored via 3% gel electrophoresis.

Library Incubation with Fibrin

Properly folded aptamer library was added to fibrin at a 200:1 aptamer to target site (defined as the site of cross-linking) ratio. A fibrin clot with 200 μL of 10 mg/mL fibrinogen (with a molecular weight of 340,000 g/mol [69]) possesses roughly 5.88×10^{-9} moles of

fibrinogen. Given fibrinogen forms a homodimer which then polymerizes into protofibrils that interact with other protofibrils to form a cross-linked fibrin fiber, the number of estimated binding sites for a 200 μL fibrin clot is $3.68*10^{-10}$ moles. Therefore, a $3.68*10^{-9}$ moles of aptamers must be added to the fibrin clot to achieve a 100:1 aptamer to target ratio. Thus, roughly 73.6 μL of 100 μM ssDNA aptamer library must be added to the fibrin clot. Incubation should be performed for 1 hour at 37°C to mimic in vivo conditions.

Removal of Unbound Aptamers

Volume remaining on top the fibrin clot after 1 hour of incubation was withdrawn via micropipette and examined via 3% gel elecrophoresis each round.

Elution and Amplification of Bound Aptamers

Fibrin clot was crushed with tweezers and digested with plasmin @ 95°C (which also permits aptamer denaturtion and unfolding). DNA mag beads were then added to the aptamer and digested fibrin solution and left to incubate for 10 minutes. The tube was then placed on a magnetic stand for 15 minutes or until the mag beads were visibly separated from the rest of the solution. The DNA attached to the mag beads was removed via micropipette and resuspended as the template in 45 μL of PCR master mix (see Table 2.4 Phusion reaction (yellow)). However, instead of using the 5'-biotin tagged forward primer and 5'-Alex647 fluorescent tagged reverse primer (as shown in Table 2.4), the primers used for PCR amplification of the aptamer library were the forward primer with no 5'-tag (5'-TCGTCGG CAGCGTCAGATGT) and the reverse primer with a 5'-phosphate tag (5'-Phosphate-GT CTCGTGGGCTCGGAGATGTG). The Phusion then Taq PCR reaction was carried out as mentioned in the dsDNA Probe Creation section. PCR parameters are also within the dsDNA Probe Creation methods section and highlighted in Table 2.2. The 85 base pair dsDNA product was purified and eluted via QIAquick Spin Column Purification Kit (as described in the dsDNA Probe Creation section).

Table 2.2: List of PCR steps and the corresponding temperatures and times within the Phusion and Taq PCR reactions.

Aptamer and Probe PCR Parameters		
PCR Step	**Temperature (°C)**	**Time (seconds)**
Denature	95	30
Anneal	50	20
Extend	68	20

Antisense Strand Digestion

The 82 base pair dsDNA PCR product included the no 5'- tag sense strand and the 5'-phosphate tagged antisense strand. Up to 5 μg of this dsDNA product was then added to a Lambda Exonuclease (New England BioLabs, Ipswich, MA, Cat. #M0262S) antisense strand digestion. The reaction set-up consisted of 5 μL of (1X) Lambda Exonuclease reaction buffer, 1 μL of 5000 units/mL Lambda Exonuclease, and water to a total volume of 50 μL. The reaction was performed at 37°C for 30 minutes. Reaction was stopped by addition of Ethylenediaminetetraacetic acid (EDTA) to 10 mM with heat inactivation at 75°for 10 minutes. Samples were then cleaned and purified via Monarch PCR DNA Cleanup Kit (New England BioLabs, Ipswich, MA, Cat. #T1030S). This was done by diluting ssDNA sample 7:1 binding buffer to sample ratio. Spin column was added to a waste collection tube. ssDNA sample diluted in binding buffer was added to the spin column and centrifuged at 15000 rpm for 1 minute. Flow-through collected in the waste tube was discarded then 200 μL of DNA wash buffer was added to the column and spun at 15000 rpm for 1 minute. Flow-through collected in the waste tube was discarded, then column was transferred to a clean 1.5 mL collection tube. 50 μL of DNA elution buffer was added to the spin column, left to sit for 1 minute, then spun at 15000 rpm for 1 minute to elute ssDNA.

Aptamer Identification

Each round the eluted ssDNA was run on a 3 % agarose gel in a well alongside the previous rounds collection. Thickness or fluorescent intensity of the band was monitored visually

or via ImageJ. Once no apparent thickness or fluorescent intensity decrease is seen, the next round of SELEX was not performed and aptamer identification via Next-Generation Sequencing (NGS) was performed. The final aptamer sequences were made compatible to the Illumina iSeq sequencer using the Illumina DNA Prep kit (Illumina, San Diego, CA, Cat. #20060060) as described in the supplier protocol. Once final-selected aptamer library were tagmented, cleaned, amplified, and diluted to the starting concentration, the sequences were ran on the iSeq. Readouts of the NGS run provided the list of the fibrin-specific aptamers.

2.1.4 CompELS

CompELS methods for discovery of a fibrin-specific aptamer are the same as the SELEX methods with two main exceptions. First, the fibrin clot is not digested as the aptamers are not to be eluted until after the final round. Second, no PCR reaction occurs until after the aptamers are eluted post-selection. Instead, the same library (at the same concentration) is added to the primary fibrin clot. Additional libraries may be synthesized and incubated with the fibrin clot during successive rounds of CompELS as this strategy requires a larger amount of library volumne (same number of aptamers with no amplification step).

2.2 Streptavidin Surface Display Design and Quantification

Three different streptavidin genes and two different surface display systems were used to design 7 different streptavidin expressing genes. These 7 constructs were ordered through IDT and are to be cloned in an E. coli vector. Primers were designed by Jessica Lin and synthesized on the ASM-2000 for Gibson assembly of plasmid constructs (see Table 2.3).

Gibson Assembly Primers
Name
Sequence

ompA_BB_His for
ACCATCATCACCACTGATAAGCTTGGCTGTTTTGGCG
ompA_BB_His rev
CGGTCATCAATTCAGCGGGGGGATC
T7Sav_ins for
CTGAATTGATGACCGGTGGCCAGC
T7Sav_ins rev
TGATGATGGTGATGCTGCTGAACTGCATCCAGC
ompA_BB_His rev
TTCCTGGCCAATTCAGCGGGGGGATC
dc_avidin_INS for
CTGAATTGGCCAGGAAGAGGACCCAG
dc_avidin_INS rev
TGATGATGGTGATGCTCTGAAAACTTCCAATTGACGG
ompA_BB_His rev
TTCCTGGCCAATTCAGCGGGGGGATC
sc_avidin_INS for
CTGAATTGGCCAGGAAGAGGACCCAG
sc_avidin_INS rev
TGATGATGGTGATGCTCTGAAAACTTCCAATTGACGG
pAIDA_BB for
TTCAGCAGTCTAGAGTGAATAACAATGGAAGCA
pAIDA_BB rev
CGGTCATATGGTGATGGTGATGGTGGT
T7Sav_ins for
ATCACCATATGACCGGTGGCCAGC

T7Sav_ins rev
CTCTAGACTGCTGAACTGCATCCAGC
pAIDA_BB for
TCAGAGTCTAGAGTGAATAACAATGGAAGC
pAIDA_BB rev
TCCTGGCATGGTGATGGTGATGGTGG
dc_avidin_ins for
ATCACCATGCCAGGAAGAGGACCCA
dc_avidin_ins rev
CACTCTAGACTCTGAAAACTTCCAATTGACG
pRSFDuet_BB for
CTGATAAAGCCAGGATCCGAATTCG
pRSFDuet_BB rev
TTGCCATGGTATATCTCCTTATTAAAGTTAAACA
pRSFDuet_ompA_StA_Ins for
GATATACCATGGCAAAAAAGACAGCTATCG
pRSFDuet_ompA_StA_Ins rev
ATCCTGGCTTTATCAGTGGTGATGATGGTGA
pRSFDuet_BB_His for
ACCATCATCACCACTGATAAAGCCAGGATCCGAATTCG
pRSF_Duet_BB for
ATAATGAAGCCAGGATCCGAATTCG
pRSF_Duet_BB rev
CCGGTCATGTGGTGATGATGGTGATGGC
AIDA1_T7Sav_ins for
CACATGACCGGTGGCCAGC

AIDA1_T7Sav_ins rev
CCTGGCTTCATTATCAGAAGCTGTATTTTATCCC
pRSF_Duet_BB rev
TTCCTGGCGTGGTGATGATGGTGATGGC
AIDA1_dc_avidin_ins for
ATCACCACGCCAGGAAGAGGACCCA
pRSF_Duet_BB rev
GCTTTCATGCTGCTGCCCATGGTATAT
lppOmpA for
CAGCAGCATGAAAGCGACCAAACTGG
lppOmpA rev
CGGTCATGCTAGCTCCGGTCGCAATTT
T7Sav for
GCTAGCATGACCGGTGGCCAGCAG
T7Sav rev
TGATGATGGTGATGCTGCTGAACTGCATCCAGCGG
lppOmpA rev
TCCTGGCGCTAGCTCCGGTCGCAATTT
dc_avidin for
AGCTAGCGCCAGGAAGAGGACCCA
dc_avidin rev
GTGATGATGGTGATGCTCTGAAAACTTCCAATTGACG

Table 2.3: Primers designed by Jessica Lin for cloning streptavidin surface display system into bacterial vector.

Streptavidin Genes

Three different streptavidin genes were used within two different surface display systems; one monovalent, one divalent, and one tetravalent.

The monovalent streptavidin had the following sequence: ATGACCGGTGGCCAGC AGATGGGTCGTGATCAGGCAGGTATTACCGGCACCTGGTATAATCAGCTGGG TAGCACCTTTATTGTTACCGCAGGCGCAGATGGTGCACTGACCGGTACGTATG AAAGCGCAGTTGGTAATGCAGAAAGCCGTTATGTTCTGACAGGTCGTTATGA TAGCGCACCGGCAACCGATGGTAGCGGCACCGCACTGGGTTGGACCGTTGCA TGGAAAAATAACTATCGTAATGCACATAGCGCAACCACCTGGTCAGGTCAGT ATGTTGGTGGTGCAGAAGCACGCATTAATACCCAGTGGCTGCTGACCAGCGG CACCACCGAAGCAAATGCCTGGAAAAGCACCCTGGTTGGTCATGATACCTTT ACCAAAGTTAAACCGAGCGCAGCAAGCATTGATGCAGCAAAAAAAGCCGGT GTGAATAATGGTAATCCGCTGGATGCAGTTCAGCAGTAATAA.

The divalent streptavidin had the following sequence: GCCAGGAAGAGGACCCAG CCCACCTTTGGCTTCACCGTCAATTGGAAGTTTTCAGAGTCCACCACTGTCTTC ACGGGCCAGTGCTTCATAGACAGGAATGGGAAGGAGGTCCTGAAGACCATGT GGCTGCTGCGGTCAAGTGTTAATGACATTGGTGATGACTGGAAAGCTACCAG GGTCGGCATCAACATCTTCACTCGCCTGCGCACACAGAAGGAGGGAGGCTCC GGAGGCTCCGCCAGAAAGTGCTCGCTGACTGGGAAATGGACCAACGATCTGG GCTCCAACATGACCATCGGGGCTGTGAACAGCAGAGGTGAATTCACAGGCAC CTACATCACAGCCGTAACAGCCACATCAAATGAGATCAAAGAGTCACCACTG CATGGGACACAAAACACCATCAACAAGTCCGGCGGATCCACCACTGTCTTCA CGGGCCAGTGCTTCATAGACAGGAATGGGAAGGAGGTCCTGAAGACCATGTG GCTGCTGCGGTCAAGTGTTAATGACATTGGTGATGACTGGAAAGCTACCAGG GTCGGCATCAACATCTTCACTCGCCTGCGCACACAGAAGGAGGGAGGCTCCG GAGGCTCCGCCAGAAAGTGCTCGCTGACTGGGAAATGGACCAACGATCTGGG CTCCAACATGACCATCGGGGCTGTGAACAGCAGAGGTGAATTCACAGGCACC

TACATCACAGCCGTAACAGCCACATCAAATGAGATCAAAGAGTCACCACTGC
ATGGGACACAAAACACAATCAACAAGAGGACCCAGCCCACCTTTGGCTTCAC
CGTCAATTGGAAGTTTTCAGAG.

The tetravalent streptavidin had the following sequence: GCCAGGAAGAGGACCC
AGCCCACCTTTGGCTTCACCGTCAATTGGAAGTTTTCAGAGTCCACCACTGTC
TTCACGGGCCAGTGCTTCATAGACAGGAATGGGAAGGAGGTCCTGAAGACCA
TGTGGCTGCTGCGGTCAAGTGTTAATGACATTGGTGATGACTGGAAAGCTAC
CAGGGTCGGCATCAACATCTTCACTCGCCTGCGCACACAGAAGGAGGGAGGC
TCCGGAGGCTCCGCCAGAAAGTGCTCGCTGACTGGGAAATGGACCAACGATC
TGGGCTCCAACATGACCATCGGGGCTGTGAACAGCAGAGGTGAATTCACAGG
CACCTACATCACAGCCGTAACAGCCACATCAAATGAGATCAAAGAGTCACCA
CTGCATGGGACACAAAACACCATCAACAAGTCCGGCGGATCCACCACTGTCT
TCACGGGCCAGTGCTTCATAGACAGGAATGGGAAGGAGGTCCTGAAGACCAT
GTGGCTGCTGCGGTCAAGTGTTAATGACATTGGTGATGACTGGAAAGCTACC
AGGGTCGGCATCAACATCTTCACTCGCCTGCGCACACAGAAGGAGGGAGGCT
CCGGAGGCTCCGCCAGAAAGTGCTCGCTGACTGGGAAATGGACCAACGATCT
GGGCTCCAACATGACCATCGGGGCTGTGAACAGCAGAGGTGAATTCACAGGC
ACCTACATCACAGCCGTAACAGCCACATCAAATGAGATCAAAGAGTCACCAC
TGCATGGGACACAAAACACAATCAACAAGAGGACCCAGCCCACCTTTGGCTT
CACCGTCAATTGGAAGTTTTCAGAGGGAGGTTCCGGATCGGGATCCGGTTCTG
GAAGCGGTAGGACCCAGCCCACCTTTGGCTTCACCGTCAATTGGAAGTTTTCA
GAGTCCACCACTGTCTTCACGGGCCAGTGCTTCATAGACAGGAATGGGAAGG
AGGTCCTGAAGACCATGTGGCTGCTGCGGTCAAGTGTTAATGACATTGGTGAT
GACTGGAAAGCTACCAGGGTCGGCATCAACATCTTCACTCGCCTGCGCACAC
AGAAGGAGGGAGGCTCCGGAGGCTCCGCCAGAAAGTGCTCGCTGACTGGGA
AATGGACCAACGATCTGGGCTCCAACATGACCATCGGGGCTGTGAACAGCAG
AGGTGAATTCACAGGCACCTACATCACAGCCGTAACAGCCACATCAAATGAG

ATCAAAGAGTCACCACTGCATGGGACACAAAACACCATCAACAAGTCCGGCG
GATCCACCACTGTCTTCACGGGCCAGTGCTTCATAGACAGGAATGGGAAGGA
GGTCCTGAAGACCATGTGGCTGCTGCGGTCAAGTGTTAATGACATTGGTGATG
ACTGGAAAGCTACCAGGGTCGGCATCAACATCTTCACTCGCCTGCGCACACA
GAAGGAGGGAGGCTCCGGAGGCTCCGCCAGAAAGTGCTCGCTGACTGGGAA
ATGGACCAACGATCTGGGCTCCAACATGACCATCGGGGCTGTGAACAGCAGA
GGTGAATTCACAGGCACCTACATCACAGCCGTAACAGCCACATCAAATGAGA
TCAAAGAGTCACCACTGCATGGGACACAAAACACAATCAACAAGAGGACCC
AGCCCACCTTTGGCTTCACCGTCAATTGGAAGTTTTCAGAG.

2.2.1 Lpp-OmpA-Streptavidin Plasmid Design

Three Lpp-OmpA-Streptavidin constructs were designed for the three different streptavidin sequences (monovalent, divalent and tetravalent).

The following is the sequence for Lpp-OmpA-MonovalentSav: ATGAAAGCGACCA
AACTGGTGCTGGGCGCGGTGATTCTGGGCAGCACCCTGCTGGCGGGCTGCAG
CAGCAACGCGAAAATTGATCAGAACAACAACGGCCCGACCCATGAAAACCA
GCTGGGCGCGGGCGCGTTTGGCGGCTATCAGGTGAACCCGTATGTGGGCTTT
GAAATGGGCTATGATTGGCTGGGCCGCATGCCGTATAAAGGCAGCGTGGAAA
ACGGCGCGTATAAAGCGCAGGGCGTGCAGCTGACCGCGAAACTGGGCTATCC
GATTACCGATGATCTGGATATTTATACCCGCCTGGGCGGCATGGTGTGGCGCG
CGGATACCAAAAGCAACGTGTATGGCAAAAACCATGATACCGGCGTGAGCCC
GGTGTTTGCGGGCGGCGTGGAATATGCGATTACCCCGGAAATTGCGACCGGA
GCTAGCATGACCGGTGGCCAGCAGATGGGTCGTGATCAGGCAGGTATTACCG
GCACCTGGTATAATCAGCTGGGTAGCACCTTTATTGTTACCGCAGGCGCAGAT
GGTGCACTGACCGGTACGTATGAAAGCGCAGTTGGTAATGCAGAAAGCCGTT
ATGTTCTGACAGGTCGTTATGATAGCGCACCGGCAACCGATGGTAGCGGCAC
CGCACTGGGTTGGACCGTTGCATGGAAAAATAACTATCGTAATGCACATAGC

GCAACCACCTGGTCAGGTCAGTATGTTGGTGGTGCAGAAGCACGCATTAATA
CCCAGTGGCTGCTGACCAGCGGCACCACCGAAGCAAATGCCTGGAAAAGCAC
CCTGGTTGGTCATGATACCTTTACCAAAGTTAAACCGAGCGCAGCAAGCATTG
ATGCAGCAAAAAAAGCCGGTGTGAATAATGGTAATCCGCTGGATGCAGTTCA
GCAG.

The following is the sequence for Lpp-OmpA-DivalentSav: ATGAAAGCGACCAAA
CTGGTGCTGGGCGCGGTGATTCTGGGCAGCACCCTGCTGGCGGGCTGCAGCA
GCAACGCGAAAATTGATCAGAACAACAACGGCCCGACCCATGAAAACCAGCT
GGGCGCGGGCGCGTTTGGCGGCTATCAGGTGAACCCGTATGTGGGCTTTGAA
ATGGGCTATGATTGGCTGGGCCGCATGCCGTATAAAGGCAGCGTGGAAAACG
GCGCGTATAAAGCGCAGGGCGTGCAGCTGACCGCGAAACTGGGCTATCCGAT
TACCGATGATCTGGATATTTATACCCGCCTGGGCGGCATGGTGTGGCGCGCGG
ATACCAAAAGCAACGTGTATGGCAAAAACCATGATACCGGCGTGAGCCCGGT
GTTTGCGGGCGGCGTGGAATATGCGATTACCCCGGAAATTGCGACCGGAGCT
AGCGCCAGGAAGAGGACCCAGCCCACCTTTGGCTTCACCGTCAATTGGAAGT
TTTCAGAGTCCACCACTGTCTTCACGGGCCAGTGCTTCATAGACAGGAATGGG
AAGGAGGTCCTGAAGACCATGTGGCTGCTGCGGTCAAGTGTTAATGACATTG
GTGATGACTGGAAAGCTACCAGGGTCGGCATCAACATCTTCACTCGCCTGCG
CACACAGAAGGAGGGAGGCTCCGGAGGCTCCGCCAGAAAGTGCTCGCTGACT
GGGAAATGGACCAACGATCTGGGCTCCAACATGACCATCGGGGCTGTGAACA
GCAGAGGTGAATTCACAGGCACCTACATCACAGCCGTAACAGCCACATCAAA
TGAGATCAAAGAGTCACCACTGCATGGGACACAAAACACCATCAACAAGTCC
GGCGGATCCACCACTGTCTTCACGGGCCAGTGCTTCATAGACAGGAATGGGA
AGGAGGTCCTGAAGACCATGTGGCTGCTGCGGTCAAGTGTTAATGACATTGG
TGATGACTGGAAAGCTACCAGGGTCGGCATCAACATCTTCACTCGCCTGCGC
ACACAGAAGGAGGGAGGCTCCGGAGGCTCCGCCAGAAAGTGCTCGCTGACTG
GGAAATGGACCAACGATCTGGGCTCCAACATGACCATCGGGGCTGTGAACAG

CAGAGGTGAATTCACAGGCACCTACATCACAGCCGTAACAGCCACATCAAAT
GAGATCAAAGAGTCACCACTGCATGGGACACAAAACACCATCAACAAGAGG
ACCCAGCCCACCTTTGGCTTCACCGTCAATTGGAAGTTTTCAGAG.

The following is the sequence for Lpp-OmpA-TetravalentSav: ATGAAAGCGACCA
AACTGGTGCTGGGCGCGGTGATTCTGGGCAGCACCCTGCTGGCGGGCTGCAG
CAGCAACGCGAAAATTGATCAGAACAACAACGGCCCGACCCATGAAAACCA
GCTGGGCGCGGGCGCGTTTGGCGGCTATCAGGTGAACCCGTATGTGGGCTTT
GAAATGGGCTATGATTGGCTGGGCCGCATGCCGTATAAAGGCAGCGTGGAAA
ACGGCGCGTATAAAGCGCAGGGCGTGCAGCTGACCGCGAAACTGGGCTATCC
GATTACCGATGATCTGGATATTTATACCCGCCTGGGCGGCATGGTGTGGCGCG
CGGATACCAAAAGCAACGTGTATGGCAAAAACCATGATACCGGCGTGAGCCC
GGTGTTTGCGGGCGGCGTGGAATATGCGATTACCCCGGAAATTGCGACCGGA
GCTAGCGCCAGGAAGAGGACCCAGCCCACCTTTGGCTTCACCGTCAATTGGA
AGTTTTCAGAGTCCACCACTGTCTTCACGGGCCAGTGCTTCATAGACAGGAAT
GGGAAGGAGGTCCTGAAGACCATGTGGCTGCTGCGGTCAAGTGTTAATGACA
TTGGTGATGACTGGAAAGCTACCAGGGTCGGCATCAACATCTTCACTCGCCTG
CGCACACAGAAGGAGGGAGGCTCCGGAGGCTCCGCCAGAAAGTGCTCGCTG
ACTGGGAAATGGACCAACGATCTGGGCTCCAACATGACCATCGGGGCTGTGA
ACAGCAGAGGTGAATTCACAGGCACCTACATCACAGCCGTAACAGCCACATC
AAATGAGATCAAAGAGTCACCACTGCATGGGACACAAAACACCATCAACAA
GTCCGGCGGATCCACCACTGTCTTCACGGGCCAGTGCTTCATAGACAGGAAT
GGGAAGGAGGTCCTGAAGACCATGTGGCTGCTGCGGTCAAGTGTTAATGACA
TTGGTGATGACTGGAAAGCTACCAGGGTCGGCATCAACATCTTCACTCGCCTG
CGCACACAGAAGGAGGGAGGCTCCGGAGGCTCCGCCAGAAAGTGCTCGCTG
ACTGGGAAATGGACCAACGATCTGGGCTCCAACATGACCATCGGGGCTGTGA
ACAGCAGAGGTGAATTCACAGGCACCTACATCACAGCCGTAACAGCCACATC
AAATGAGATCAAAGAGTCACCACTGCATGGGACACAAAACACCATCAACAA

GAGGACCCAGCCCACCTTTGGCTTCACCGTCAATTGGAAGTTTTCAGAGGGA
GGTTCCGGATCGGGATCCGGCTCTGGCAGCGGCAGGACCCAGCCCACCTTTG
GCTTCACCGTCAATTGGAAGTTTTCAGAGTCCACCACTGTCTTCACGGGCCAG
TGCTTCATAGACAGGAATGGGAAGGAGGTCCTGAAGACCATGTGGCTGCTGC
GGTCAAGTGTTAATGACATTGGTGATGACTGGAAAGCTACCAGGGTCGGCAT
CAACATCTTCACTCGCCTGCGCACACAGAAGGAGGGAGGCTCCGGAGGCTCC
GCCAGAAAGTGCTCGCTGACTGGGAAATGGACCAACGATCTGGGCTCCAACA
TGACCATCGGGGCTGTGAACAGCAGAGGTGAATTCACAGGCACCTACATCAC
AGCCGTAACAGCCACATCAAATGAGATCAAAGAGTCACCACTGCATGGGACA
CAAAACACCATCAACAAGTCCGGCGGATCCACCACTGTCTTCACGGGCCAGT
GCTTCATAGACAGGAATGGGAAGGAGGTCCTGAAGACCATGTGGCTGCTGCG
GTCAAGTGTTAATGACATTGGTGATGACTGGAAAGCTACCAGGGTCGGCATC
AACATCTTCACTCGCCTGCGCACACAGAAGGAGGGAGGCTCCGGAGGCTCCG
CCAGAAAGTGCTCGCTGACTGGGAAATGGACCAACGATCTGGGCTCCAACAT
GACCATCGGGGCTGTGAACAGCAGAGGTGAATTCACAGGCACCTACATCACA
GCCGTAACAGCCACATCAAATGAGATCAAAGAGTCACCACTGCATGGGACAC
AAAACACCATCAACAAGAGGACCCAGCCCACCTTTGGCTTCACCGTCAATTG
GAAGTTTTCAGAG.

2.2.2 pAIDA1 Plasmid Design

A variation of the AIDA surface expression system, originally displaying a passenger protein flanked by His and Myc tags [70], was designed to display either divalent (pAIDA1-DivalentSav) or tetravalent (pAIDA-TetravalentSav) streptavidin with a Myc tag. The following is the sequence for pAIDA1-DivalentSav-Myc: ATGAATAAGGCCTACAGTAT
CATTTGGAGCCACTCCAGACAGGCCTGGATTGTGGCCTCAGAGTTAGCCAGA
GGACATGGTTTTGTCCTTGCAAAAAATACACTGCTGGTATTGGCGGTTGTTTC
CACAATCGGAAATGCATTTGCAGTCGACATGGCAGAGGCGGGGATCACGGGG

ACGTGGTACAACCAATTGGGCACGACGTTCATAGTCACGGCTGGTGCCGATG
GGGCGTTGACCGGAACTTACGAATGCGCGGTAGGGAATGCGGAGAGTAGGTA
TGTGCTGACCGGTAGGTACGACACCGCGCCCGCGACAGATGGGAGCGGCACC
GCCTTTGGCTGGACCGTCGCATGGAAGAACAATTACAGCGCTCATAGCGCGA
CTACCTGGACCGGCCAGTATGTCGGAGGAGCCGAAGCTAGGATTAACACACA
GTGGTTCCTGACCACTGGTACGACAGAAGCGAACGCGTGGACGACGCTGGTA
GGACATGATACGTTCACCAAAGTGAAGCCGACCGCTGCTAGTGAAGAAGAAG
AAGAAGAACTGGAAGCGCTGTTCCAGGGTCCGGGTACCCAGAAACAGCGTAC
CGAGCTCGAAAACCTGTACTTCCAGGGTGAACAGAAACTGATTAGCGAAGAA
GATCTGTCTAGAGTGAATAACAATGGAAGCATTGTCATTAATAACAGCATTA
TAAACGGGAATATTACGAATGATGCTGACTTAAGTTTTGGTACAGCAAAGCT
GCTCTCTGCTACAGTGAATGGTAGTCTTGTTAATAACAAAAATATCATTCTTA
ATCCTACAAAAGAAAGTGCGGCCGCTATAGGTAATACTCTTACCGTGTCAAA
TTATACTGGGACACCGGGAAGTGTTATTTCTCTTGGTGGTGTGCTTGAAGGAG
ATAATTCACTTACGGACCGTCTGGTGGTGAAAGGTAATACCTCTGGTCAAAGT
GACATCGTTTATGTCAATGAAGATGGCAGTGGTGGTCAGACGAGAGATGGTA
TTAATATTATTTCTGTAGAGGGAAATTCTGATGCAGAATTCTCTCTGAAGAAC
CGCGTAGTTGCCGGAGCTTATGATTACACACTGCAGAAAGGAAACGAGAGTG
GGACAGATAATAAGGGATGGTATTTAACCAGTCATCTTCCCACATCTGATACC
CGGCAATACAGACCGGAGAACGGAAGTTATGCTACCAATATGGCACTGGCTA
ACTCACTGTTCCTCATGGATTTGAATGAGCGTAAGCAATTCAGGGCCATGAGT
GATAATACACAGCCTGAGTCTGCATCCGTGTGGATGAAGATCACTGGAGGAA
TAAGCTCTGGTAAGCTGAATGACGGGCAAAATAAAACAACAACCAATCAGTT
TATCAATCAGCTCGGGGGGGATATTTATAAATTCCATGCTGAACAACTGGGTG
ATTTTACCTTAGGGATTATGGGAGGATACGCGAATGCAAAAGGTAAAACGAT
AAATTACACGAGCAACAAAGCTGCCAGAAACACACTGGATGGTTATTCTGTC
GGGGTATACGGTACGTGGTATCAGAATGGGGAAAATGCAACAGGGCTCTTTG

CTGAAACTTGGATGCAATATAACTGGTTTAATGCATCAGTGAAAGGTGACGG
ACTGGAAGAAGAAAAATATAATCTGAATGGTTTAACCGCTTCTGCAGGTGGG
GGATATAACCTGAATGTGCACACATGGACATCACCTGAAGGAATAACAGGTG
AATTCTGGTTACAGCCTCATTTGCAGGCTGTCTGGATGGGGGTTACACCGGAT
ACACATCAGGAGGATAACGGAACGGTGGTGCAGGGAGCAGGGAAAAATAAT
ATTCAGACAAAAGCAGGTATTCGTGCATCCTGGAAGGTGAAAAGCACCCTGG
ATAAGGATACCGGGCGGAGGTTCCGTCCGTATATAGAGGCAAACTGGATCCA
TAACACTCATGAATTTGGTGTTAAAATGAGTGATGACAGCCAGTTGTTGTCAG
GTAGCCGAAATCAGGGAGAGATAAAGACAGGTATTGAAGGGGTGATTACTCA
AAACTTGTCAGTGAATGGCGGAGTCGCATATCAGGCAGGAGGTCACGGGAGC
AATGCCATCTCCGGAGCACTGGGGATAAAATACAGCTTCTGA.

The following is the sequence for pAIDA1-TetravalentSav-Myc: ATGAATAAGGC
CTACAGTATCATTTGGAGCCACTCCAGACAGGCCTGGATTGTGGCCTCAGAGT
TAGCCAGAGGACATGGTTTTGTCCTTGCAAAAAATACACTGCTGGTATTGGCG
GTTGTTTCCACAATCGGAAATGCATTTGCAGTCGACATGCGTAAAATCGTTGT
TGCGGCGATCGCGGTTTCTCTGACCACCGTTTCTATCACCGCGTCTGCGTCTG
CGGACCCGTCTAAAGACTCTAAAGCGCAGGTTTCTGCGGCGGAAGCGGGTAT
CACCGGTACCTGGTACAACCAGCTGGGTTCTACCTTCATCGTTACCGCGGGTG
CGGACGGTGCGCTGACCGGTACCTACGAATCTGCGGTTGGTAACGCGGAATC
TCGTTACGTTCTGACCGGTCGTTACGACTCTGCGCCGGCGACCGACGGTTCTG
GTACCGCGCTGGGTTGGACCGTTGCGTGGAAAAACAACTACCGTAACGCGCA
CTCTGCGACCACCTGGTCTGGTCAGTACGTTGGTGGTGCGGAAGCGCGTATCA
ACACCCAGTGGCTGCTGACCTCTGGTACCACCGAAGCGAACGCGTGGAAATC
TACCCTGGTTGGTCACGACACCTTCACCAAAGTTAAACCGTCTGCGGCGTCTA
TCGACGCGGCGAAAAAAGCGGGTGTTAACAACGGTAACCCGCTGGACGCGG
TTCAGCAGCTGGAAGCGCTGTTCCAGGGTCCGGGTACCCAGAAACAGCGTAC
CGAGCTCGAAAACCTGTACTTCCAGGGTGAACAGAAACTGATTAGCGAAGAA

GATCTGTCTAGAGTGAATAACAATGGAAGCATTGTCATTAATAACAGCATTA
TAAACGGGAATATTACGAATGATGCTGACTTAAGTTTTGGTACAGCAAAGCT
GCTCTCTGCTACAGTGAATGGTAGTCTTGTTAATAACAAAAATATCATTCTTA
ATCCTACAAAAGAAAGTGCGGCCGCTATAGGTAATACTCTTACCGTGTCAAA
TTATACTGGGACACCGGGAAGTGTTATTTCTCTTGGTGGTGTGCTTGAAGGAG
ATAATTCACTTACGGACCGTCTGGTGGTGAAAGGTAATACCTCTGGTCAAAGT
GACATCGTTTATGTCAATGAAGATGGCAGTGGTGGTCAGACGAGAGATGGTA
TTAATATTATTTCTGTAGAGGGAAATTCTGATGCAGAATTCTCTCTGAAGAAC
CGCGTAGTTGCCGGAGCTTATGATTACACACTGCAGAAAGGAAACGAGAGTG
GGACAGATAATAAGGGATGGTATTTAACCAGTCATCTTCCCACATCTGATACC
CGGCAATACAGACCGGAGAACGGAAGTTATGCTACCAATATGGCACTGGCTA
ACTCACTGTTCCTCATGGATTTGAATGAGCGTAAGCAATTCAGGGCCATGAGT
GATAATACACAGCCTGAGTCTGCATCCGTGTGGATGAAGATCACTGGAGGAA
TAAGCTCTGGTAAGCTGAATGACGGGCAAAATAAAACAACAACCAATCAGTT
TATCAATCAGCTCGGGGGGGATATTTATAAATTCCATGCTGAACAACTGGGTG
ATTTTACCTTAGGGATTATGGGAGGATACGCGAATGCAAAAGGTAAAACGAT
AAATTACACGAGCAACAAAGCTGCCAGAAACACACTGGATGGTTATTCTGTC
GGGGTATACGGTACGTGGTATCAGAATGGGGAAAATGCAACAGGGCTCTTTG
CTGAAACTTGGATGCAATATAACTGGTTTAATGCATCAGTGAAAGGTGACGG
ACTGGAAGAAGAAAAATATAATCTGAATGGTTTAACCGCTTCTGCAGGTGGG
GGATATAACCTGAATGTGCACACATGGACATCACCTGAAGGAATAACAGGTG
AATTCTGGTTACAGCCTCATTTGCAGGCTGTCTGGATGGGGGTTACACCGGAT
ACACATCAGGAGGATAACGGAACGGTGGTGCAGGGAGCAGGGAAAAATAAT
ATTCAGACAAAAGCAGGTATTCGTGCATCCTGGAAGGTGAAAAGCACCCTGG
ATAAGGATACCGGGCGGAGGTTCCGTCCGTATATAGAGGCAAACTGGATCCA
TAACACTCATGAATTTGGTGTTAAAATGAGTGATGACAGCCAGTTGTTGTCAG
GTAGCCGAAATCAGGGAGAGATAAAGACAGGTATTGAAGGGGTGATTACTCA

AAACTTGTCAGTGAATGGCGGAGTCGCATATCAGGCAGGAGGTCACGGGAGC
AATGCCATCTCCGGAGCACTGGGGATAAAATACAGCTTCTGA.

2.2.3 dsDNA Probe Creation

Polymerase Chain Reaction (PCR) was performed to create the dsDNA probes. A 20 nucleotide long forward primer with a 5' biotin tag (5'Biotin-TCGTCGGCAGCGTCAGATGT) and a 22 nucleotide long reverse primer with 5' Alex647 fluorescent tag (5'Alex647-GTCTCGTGGGCTCGGAGATGTG) were used as primers for the PCR reaction. Primers were diluted from a 100 μM concentration to 5 μM concentration. A total volume of 1.8 mL of Phusion mastermix and 264 μL of Taq mastermix was made (see Table 2.4). The dsDNA probe PCR reaction occurred in two separate PCR reactions.

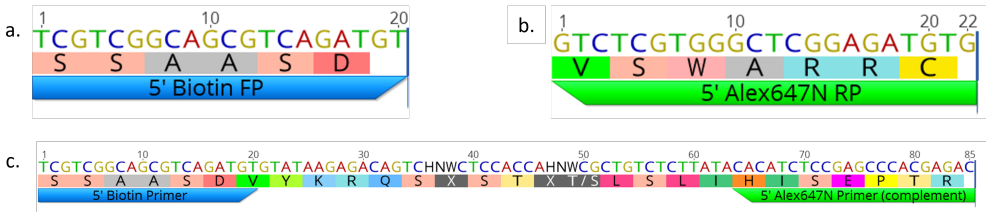

Figure 2.1: 20 nucleotide long 5'-biotin labelled forward primer, 22 nucleotide long 5'-Alex647 fluorescently labelled reverse primer, and 85 nucleotide long template designs.

First, 45 μL of Phusion master mix was added to 5 μL of 100 μM template DNA of 85 nucleotides (TCGTCGGCAGCGTCAGATGTGTATAAGAGACAGTCHNWCTCCACCAH-NWCGCTGTCTCTTATACACATCTCCGAGCCCACGAGAC). This sequence was designed to allow binding of the binding and extension of 5'-Alex647 labelled reverse primer during the first cycle of PCR. The Phusion PCR cycle settings are as follows: 20 cycles of denature at 95°C for 30 seconds, anneal at 50°C for 20 seconds, and extension at 68°C at 20 seconds.

The second reaction includes adding 2 μL of Taq mastermix (see Table 2.4 to the reaction tubes from the first (Phusion reaction tubes). The Taq PCR cycle settings are as follows: 20 cycles of denature at 95°C for 30 seconds, anneal at 50°C for 20 seconds, and

extension at 68°C at 20 seconds.

Table 2.4: dsDNA probe PCR reaction setup. 45 μL of Phusion master mix was added to 5 μL of template DNA for the first reaction. Then, 2 μL of Taq master mix was added to Phusion PCR product for the second reaction.

dsDNA Probe PCR Setup		
Reagent	**Volume (μL)**	
5x Phusion HF rxn buffer	360	Phusion Reaction (first)
5 μM Forward Primer (biotinylated)	180	
5 μM Reverse Primer (fluorescent)	180	
100 nM template	0*	
dNTP mix (10 mM each)	36	
DMSO	36	
Phusion	6	
Water	800	
dNTP mix (10 mM each)	60	Taq Reaction (second)
Taq Polymerase	24	
Water	160	

The dsDNA PCR product must be purified prior to use in flow cytometry. The QIAquick Spin Column Purification Kit (Qiagen, Hilden, Germany, Cat #28104) was used to isolate the dsDNA probe from the remaining PCR reagents. The amount of PCR reactions added per spin column was examined and noticeable yield dropoff was seen when adding more than one PCR reaction to a single QIAquick spin column (see Table 2.5). 15 μL of PB buffer was added to the membrane of the QIAquick spin columns. The 50 μL PCR reaction was mixed with 250 μL of PB buffer and transferred to the spin column. Spin column was transferred a centrifuge and spun at 15000 rpm for 1 minute. The spin column was then washed with 750 μ of PE buffer and centrifuged again at 15000 rpm for 1 minute. Elution buffer (EB) was heated via 15 seconds in the microwave then 50 μL was added to the spin column. After 2 minutes of incubation, the spin column was placed in a collected tube and centrifuged at 15000 rpm for 1 minute.

Table 2.5: Optimization of number of PCR reactions (50 μL per reaction) to add to QIAquick spin columns.

of Samples per spin column	**Mix**	**Streptavidin Mag Bead Volume (10 mg/mL)**	**dsDNA Concentration (ng/uL)**
1	Sample: 50 uL Wash: 250 uL PB Elute: 50 uL EB	5	93.53
2	Sample: 100 uL Wash: 500 uL PB Elute: 50 uL EB	5	120.76

dsDNA Probe Calibration with Streptavidin Mag Beads

To quantify the amount of E. coli streptavidin expression levels with the biotinylated dsDNA probe, the fluorescence during flow cytometry needed to be calibrated. This was done by incubating the dsDNA probe with 10 mg/mL Streptavidin Magnetic Beads (Pierce Biotechnology, Rockford, IL, Cat. #88816). The dsDNA probe concentration was measured at 92.99 ng/μL prior to incubation with the streptavidin mag beads. An array of 3 different working concentrations were tested along with one control (see Table 2.6.

Table 2.6: Array of different biotin and fluorescent labelled probe dilutions incubated with streptavidin mag beads.

Condition (Probe dilution)	**dsDNA Probe Volume (92.99 ng/uL)**	**PBS Volume**	**Streptavidin Mag Bead Volume (10 mg/mL)**
Control	0	100	5
1 (1:10 dilution)	10	90	5
2 (1:1 dilution)	50	50	5
3 (none)	100	0	5

2.2.4 dsDNA Probe-Cell Conjugation

Cell Preparation

Frozen overnight culture of transformed BL21 cells were thawed. The cells were diluted or incubated at 37 to achieve an OD600 of 0.8 $\pm$ 0.2. Cell were then induced with 1:100 addition of IPTG (or not induced for a negative control). After induction, eppendorf tubes were centrifuged to pellet cells. Super optimal broth (SOB) media was discarded and cells were resuspended in the appropriate amount of PBS to achieve the following OD600 values: 0.125 (10^8 cells/mL), 0.0125 (10^7 cells/mL), 0.00125 (10^6 cells/mL), and 0.000125 (10^5 cells/mL). The actual OD600 values cell concentration were measured: 0.135 (1.08*10^8 cells/mL), 0.0133 (1.06*10^7 cells/mL), 0.0048 (3.84*10^6 cells/mL), and 0.0008 (6.4*10^5 cells/mL), respectively (see Table 2.7). Values were achieved by performing 9:1 serial dilutions. 1 mL of each tube (labeled 1-4) was transferred to a clean 2 mL eppendorf tube. 60 μL of 77 ng/μL dsDNA probe was added to each tube and left to incubate for 1 hour. After incubation, tubes were centrifuged at 2000 rpm for 5 minutes to pellet the cell:probe mix. Supernatant was discarded and cell:probe mix was resuspended in 1 mL of PBS then transferred to a falcon tube for flow cytometry.

Table 2.7: Gradient of cell concentrations prior to incubation with dsDNA probe.

Cell Concentrations for dsDNA Probe Conjugation				
	1	**2**	**3**	**4**
Ideal OD600	0.125	0.0125	0.00125	0.000125
Ideal Cell Concentration (Cells/mL)	1e8	1e7	1e6	1e5
Actual OD600	0.135	0.0133	0.0048	0.0008
Actual Cell Concentration (Cells/mL)	1.08e8	1.06e7	3.84e6	6.4e5

Streptavidin mag beads were used as a positive control within the dsDNA probe-cell conjugation experiment. 5 μL and 2 μL were added to 1 mL of PBS. 84 μL of 57 ng/μL

ds DNA probe was added to the beads in PBS and incubated for 1 hour. Tubes were then applied to a magnetic stand and clear supernatant was discarded. Tube were removed from magnetic stand and bead:probe conjugates were resuspended in a total of 1 mL of PBS and transferred to a falcon tube for flow cytometry.

CHAPTER 3

RESULTS

3.1 Fibrin Clot Formation

Of the 6 incubation combinations between 10 mg/mL fibrinogen and 1 kU/mL thrombin with 2 μL mg/uL factor XIII and 2 L of $CaCl_2$, five (tubes 1, 2, 3, 5, and 6) combinations formed solidified clots (see Figure 3.1a.) while one (tube 4) combination remained mostly aqueous with little to no coagulation. Solidified fibrin clots possessed an opaque coloring, differing from the clear aqueous substituents. Of the five solidified clots, one clot (tube 5) showed significantly stronger structural integrity capable of not dissolving when water was added (see Figure 3.1b.).

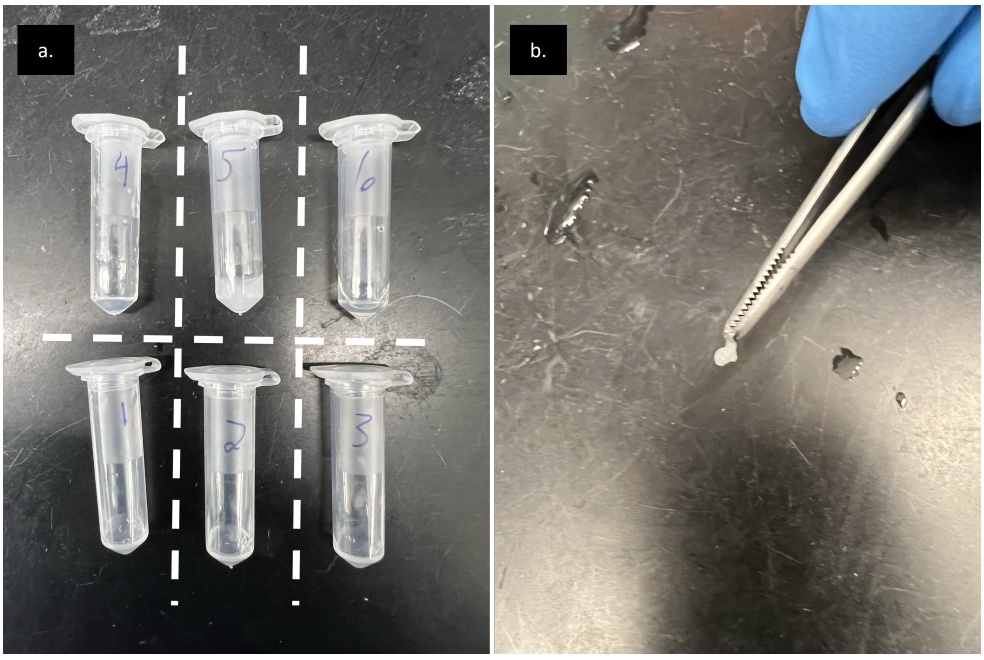

Figure 3.1: (a.-b.) 6 different clots were formed to determine the optimal ratio of 10 mg/mL fibrinogen and 1 kU/mL thrombin. a.) Tubes 1, 2, 3, 5, and 6 formed solidified clot structure. Tube number 5 showed the most coagulation. b.) Tube number 5 showed the most coagulation and obtained an indissoluble structure.

3.2 Solid-Phase Synthesis

3.2.1 Library Synthesis

The 82 nucleotide long ssDNA library had a resulting concentration 2301 ng/μL (91.42 μM). The HPLC data of the ssDNA library showed distinguishable peaks at minutes 1, 8.5, and 12. The max peaks (at minute 8.5) for the 82 nucleotide ssDNA library and 80 nucleotide long reference ssDNA were 88.32 and 168.92, respectively (see Figure 3.2). Noticeably higher peaks are seen within the ssDNA library graph at minutes 1 and 12.

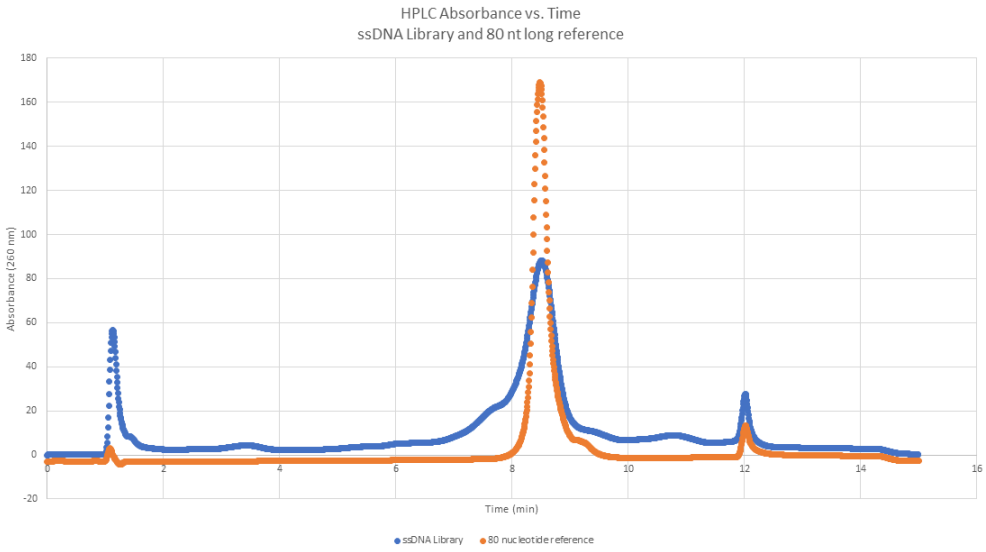

Figure 3.2: Absorbance @ 260 nanometers versus time graph of 82 nucleotide long ssDNA library and 80 nucleotide long reference ssDNA oligonucleotide. Peaks with different amplitudes seen for both at minutes 1, 8.5, and 12.

3.2.2 Phosphorylated Primer Synthesis

The 23 nucleotide long phosphorylated primer, synthesized alongside 4 standard DNA primers not used within the scope of this project, showed consistent, but light titryl collection during the 1st, 13th, and 22nd rounds of the solid-phase DNA synthesis (see Figure 3.3. The titryl collection during the 23rd (last) round of solid-phase DNA synthesis appears

clear and completely transparent. The titryl collection during the synthesis of the standard DNA primers appeared a consistent yellow-brown color Compared the nearly transparent titryl collection from the phosphorylated oligonucleotide.

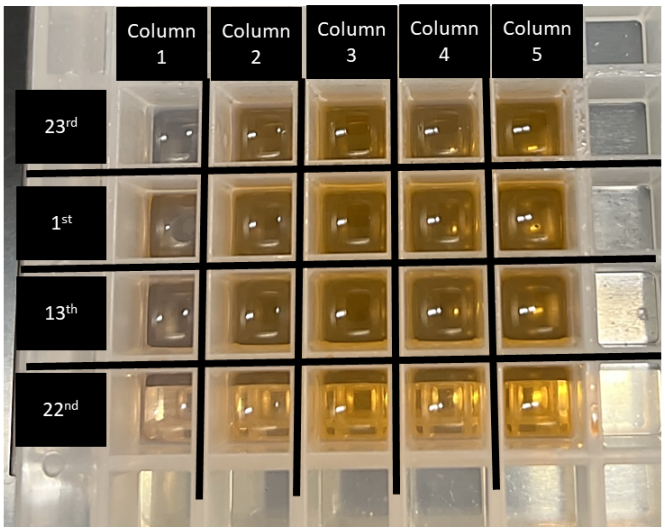

Figure 3.3: Titrl collection from the 1st, 13th, 22nd, and 23rd cycles from the solid-phase DNA synthesis of the phosphorylated DNA primer (column 1) and standard DNA primers (columns 2-5). Apparent color differences between the phosphorylated oligonucleotide titryl collection (very light, almost clear, inconsistent final step) and the standard DNA oligonucleotide titryl collections (consistent yellow-brown.

The phosphorylated and non-phosphorylated ssDNA primers resuspended in 50 μL of 10 mM Tris HCl with 50% glycerol had a measured concentration 1307.01 ng/μL (186.84 μM) and 734.1 ng/μL (106.36 μM), respectively. 43.42 μL and 3.19 ng/μL, respectively, of the 10 mM Tris HCl with 50% glycerol was added to dilute the primers to 100 μM. The high performance liquid chromatography (HPLC) data of phosphorylated and non-phosphorylated primers showed all the same absorbance peaks at roughly minute 1, 10, and 12. Compared to the control, both phosphorylated and non-phosphorylated oligonucleotides showed differing absorbance peaks at minute 1 and minute 10, while following the same peak as the control at minute 12 (see Figure 3.4a.). The waveform of the phosphorylated and non-phosphorylated ssDNA absorbance peaks match almost identically, however

the amplitudes are different. The amplitude of the absorbance peak waveform of the phosphorylated and non-phosphorylated primer had an absorbance of 12.45 nm and 31.17 nm, respectively. The amplitude of the phosphorylated, non-phosphorylated, and buffer peaks at minute 12 are all within ± 0.5 nanometers (see Figure 3.4b.).

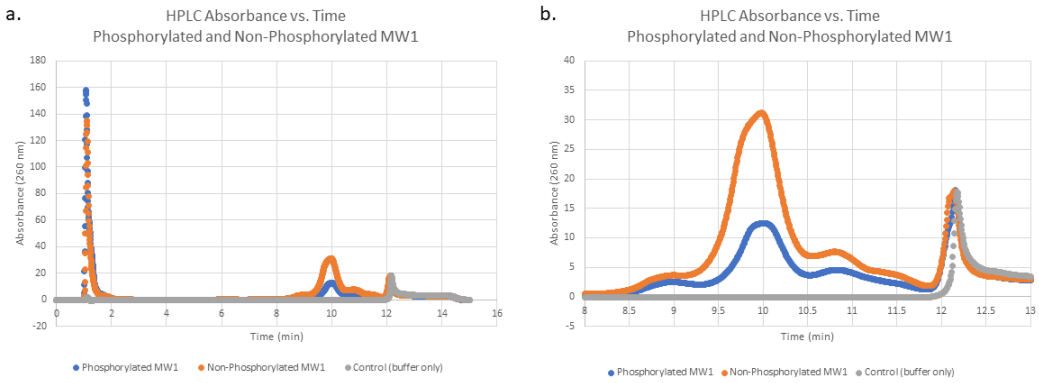

Figure 3.4: Absorbance @ 260 nanometers versus time graph. a.) 3 peaks seen at minutes 1, 10, and 12. Samples show distinguishable peaks at minute 1 but indistinguishable peaks at minute 12. b.) Zoomed in view of peaks at minutes 10 and 12. b.) Non-phosphorylated and phosphorylated oligonucleotides show the same shape but different amplitudes at 10 minute peak.

3.3 Streptavidin Surface Display

3.3.1 dsDNA Probe Creation

After purification via the QIAquick spin columns, the resulting dsDNA concentration of the 5'-biotin and 5'-Alex647 labelled dsDNA probe was measured to be 92.99 ng/μL (see Figure 3.6). 3 % gel electrophoresis results showed strong PCR product bands slightly below the 100 base pair (bp) ladder marker along with slightly visible bands corresponding to the 85 nucleotide long template band in the adjacent well. No visible bands correspond-

ing to the 20 nucleotide long 5'-biotin tagged primer and 22 nucleotide long 5'-Alex647 fluorescent primer were seen.

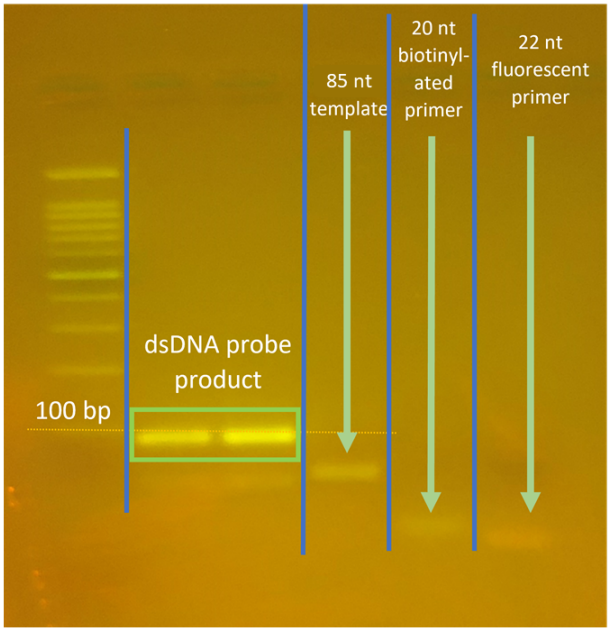

Figure 3.5: Gel including wells containing 100 bp ladder, dsDNA probe product, 85 nucleotide long template, 20 nucleotide long 5'-biotinylated forward primer, and 22 nucleotide long 5'-Alex647 fluorescent primer.

3.3.2 dsDNA Probe Calibration with Streptavidin Mag Beads

Mean fluorescence of dsDNA probe diluted in PBS 1:10 (9.30 ng/μL), 1:1 (46.50 ng/μL), and no dilution (92.99 ng/μL) was measured at 517, 2549, and 3200, respectively, with corresponding fluorescent standard deviations of 539, 3904, and 7511, respectively (see Figure 3.6). The mean fluorescence and standard deviation of the control (streptavidin beads with no dsDNA probe) was measured to be 9.39 and 53.1, respectively.

3.3.3 DNA-Cell Conjugation

Flow cytometry results for the cell concentrations of 1.08×10^8 and 1.06×10^7 cells/mL showed a mean fluorescence value of 13.7 and 51.5, respectively, with corresponding standard deviations of 130 and 330, respectively. The flow cytometry data collection for the

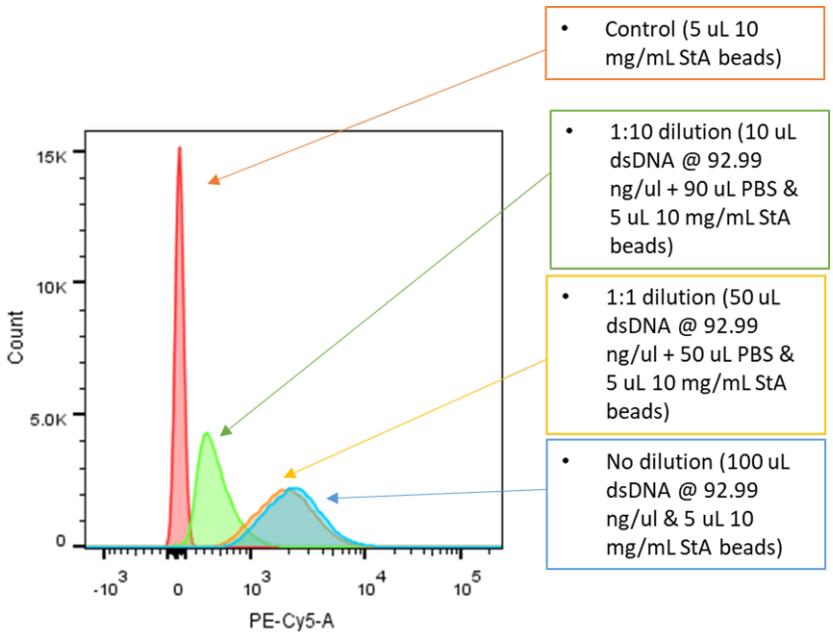

	Sample Name	Count	Mean : PE-Cy5-A	SD : PE-Cy5-A
	StA Beads w,2f, dsDNA Probe_1.fcs	100000	3200	7511
	StA Beads w,2f, dsDNA Probe_2.fcs	100000	2549	3904
	StA Beads w,2f, dsDNA Probe_3.fcs	100000	517	539
	Control StA Beads_Control.fcs	100000	9.39	53.1

Figure 3.6: Flow cytometry results of biotinylated and fluorescent dsDNA probe conjugated to streptavidin (StA) mag beads. Gradient of dsDNA probe concentrations incubated with 5 μL of 10 mg/mL StA beads. Distinguishable peaks seen for the various probe concentrations.

lower cell concentrations ($3.84\text{x}10^6$ and $6.4\text{x}10^5$) was stopped due to very low cell counts. The positive control, streptavidin mag beads, had a mean fluorescence/standard deviation value of 3439 and 3715 at $1.92\text{x}10^7$ and $4.8\text{x}10^7$ beads/mL, repectively. Corresponding standard deviation values for the streptavidin mag beads were 2235 and 2568, respectively (see Figure 3.7).

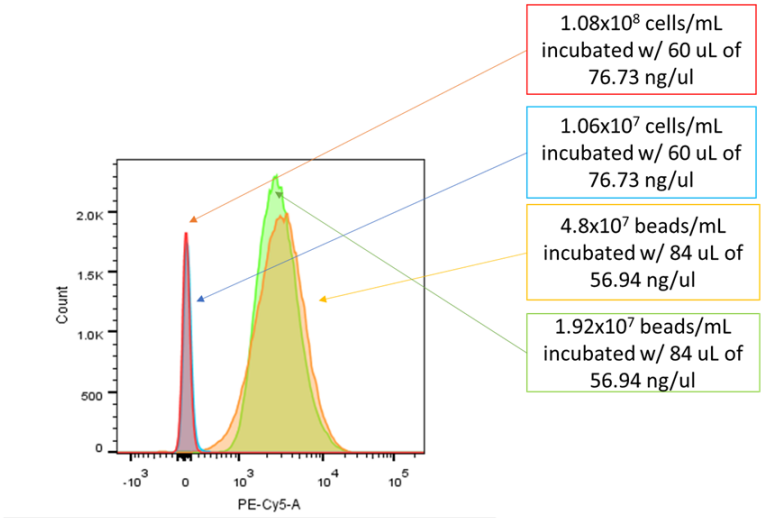

	Sample Name	Subset Name	Count	Mean : PE-Cy5-A	SD : PE-Cy5-A
	Cells_1.fcs	E. coli	14497	13.7	130
	Cells_2.fcs	E. coli	14622	51.5	330
	Mag Beads_C1.fcs	Mag Beads	99411	3715	2568
	Mag Beads_C2.fcs	Mag Beads	96114	3439	2235

Figure 3.7: Flow cytometry results of dsDNA probe incubated with cells at different concentrations. Streptavidin mag beads were utilized as a positive control.

CHAPTER 4

DISCUSSION

In this work, a fibrin clot, aptamer library, Gibson assembly primers, and dsDNA probe were created to provide the necessary components to perform SELEX and CompELS.

The solidifed, indissolvable fibrin clot (see Figure 3.1) showed significant coagulation. The cleavage of fibrinopeptides by the enzyme thrombin allowed the successful polymerization of fibrinogen into a cross-linked structure, which was further supported by factor XIII. The central E nodule is the desired target of a fibrin-specific aptamer since the N-terminals of cleaved fibrinogen are different than monomeric form of fibrinogen. Aside from this cleaved N-term, no noticable differences exist between fibrin and fibrinogen. The normal fibrinogen levels of for an adult range from 200-400 mL/dL, thus an aptamer introduced to the bloodstream in vivo would encounter a significant amount of fibrinogen. Thus, negative selection of the aptamer library against fibrinogen is a key step within the selecton process to prevent non-specific binding.

The ssDNA library with the variable region designed to minimize G-quadruplex formation, via $(\mathrm{NNNH})_1 0$ design, possesses 6.81×10^{22} sequence possibiDNA library and 80 nucleotide reference peaks at mlities. The HPLC data demonstrating matching peaks at minute 8.5 indicate a successful synthesis of the run (see Figure 3.2). The smaller peaks seen at minute 1 indicates the initial reading of the buffer. However, the profound ssDNA library peak indicates either the glycerol within the buffer or an impure sample. No ssDNA purification was performed prior to the HPLC run. Possibly, the acetonitrile washes between each step of solid-phase DNA synthesis cycle did not completely wash the unbound DNA amidites from the synthesis plate, explaining the profound peak. The skewed left bell shape of the ssDNA library peak at minute 8.5 also indicates an impure sample as oligonucleotides slightly shorter than 82 nucleotides long may have been synthesized. The short

peaks at minute 12 indicates the washing step of the HPLC run and is not related to the sample. The ssDNA library should be purified using spin columns then rerun on HPLC.

The phosphorylated primer synthesis was unsuccessful based on the titryl collection and HPLC results. No DMT group was collected on the final step of the solid-phase DNA synthesis (see Figure 3.3), indicating the addition of chemical phosphorylation reagent was not properly coupled to the 5'-end. Also, issues with the addition of normal DNA amidites likely ocurred as the DMT collection at steps 1, 13, and 22 are much lighter than the DMT collection from the standard DNA primers. The HPLC data of the phosphorylated primer compared to the non-phosphorylated version showed peaks at identical time point (minute 10; see Figure 3.4). This indicates no difference in the molecular weight of the two oligonucleotides, and, thus, no difference in DNA sequence and no addition of phosphate. There are phosphorylation kinase kits are able to ligate a phosphate group to the 5'-end of a DNA oligo, and might be a better alternative to the chemical phosphorylation reagent used in this DNA synthesis. The amplitudes of the the two peaks correspond to the different synthesis yields as the concentration of the phosphorylated oligonucleotide was significantly lower than the non-phosphorylated version. Also, the issue of glycerol or impure sample was seen at minute 1 of this HPLC run (as it was in the ssDNA library HPLC run). ssDNA purification via spin columns should be performed then a rerun of HPLC should confirm whether the minute 1 peaks are due to the glycerol or unbound DNA amidites. Lastly, the minute 12 peaks are from the wash step of HPLC and is not related to the DNA synthesis.

Creation and functionality of the 85 bp dsDNA probe was very successful. Strong dsDNA probe product bands were seen during 3% gel electrophoresis (see Figure 3.5). No primer bands were seen indicating the PCR reaction successfully exhausted the 20 nucleotide long 5'-biotinylated primer and the 22 nucleotide long 5'-Alex647 primer. Primer exhaustion plus the strong dsDNA probe product band compared to the faint template band indicates the probe PCR reaction is nicely optimized. The 20 nucleotide 5'-biotinylated primer appears to have a slightly larger molecular weight than the 22 nucleotide long 5'-

Alex647 labelled primer. This is explained by the fact biotin has molecular weight of 244.31 g/mol [71] and Alex647 fluorophore has a molecular weight of 1.3 g/mol. Incubation of the various concentrations of dsDNA probe product with streptavidin mag beads showed a great spectrum of mean fluorescence (see Figure 3.6). Saturation of streptavidin binding sites appeared to approach saturation as the peaks between 1:1 diluted probe and non-diluted probe had noticable overlap (but still significantly different mean fluorescence, p¡0.0001). Additional probe dilutions incubated with the same streptavidin mag bead volume can provide enough data points to characterize streptavidin surface expression on E. coli cells. The attempt to characterize the streptavidin surface display on the cells proved unsuccessful as the cells did not appear to adequately express streptavidin compare to the streptavidin mag beads. Despite the apparent identical peaks between the two cell concentrations (see Figure 3.7), the $1.06x10^7$ cells/mL concentration had a significantly higher mean fluorescence than the $1.08x10^8$ cells/mL concentration (p¡0.0001). Different surface display systems with different streptavidin variations were designed to optimize the streptavidin expression. Yet, the 85 base pair dsDNA probe, of similar length as the 82 nucleotide long ssDNA aptamer, demonstrated the ability of 5'-biotinylated DNA to bind to streptavidin. This fact proves the concept of conjugating DNA to streptavidin for biotechnological approaches.

Unfortunately, SELEX and CompELS were not performed and discovery of a fibrin-specific aptamer did not occur. However, a comprehensive pipeline of methods are proposed to perform both sELEX and CompELS to identify an aptamer. Additionally, Gibson assembly of the Lpp-OmpA and pAIDA1 surface display of monovalent, divalent, and tetravalent streptavidin proteins was not yet performed. However, the provided genetic sequences for the corresponding gene constructs are provided for future experimental testing.

CHAPTER 5
CONCLUSION

Many aptamers have been discovered and synthesized for a variety of applications, especially within the coagulation pathway [72] [73] [74] [75] [76]. However, an aptamer specifically targeting fibrin has yet to be identified. The ability to add a biotin molecule to the 5'-end of ssDNA DNA, demonstrated by the dsDNA probe, allows an aptamer to tether to cells and nanoparticles expressing streptavidin. This aptamer-cell or aptamer-nanoparticle conjugation allows the aptamer to function as a targeted delivery agent, much like antibody conjugated nanoparticles. In the context of this work, SELEX and CompELS strategies to identify a fibrin-specific aptamer were described. Upon the identification of a fibrin-specific aptamer, a 5'-biotin molecule. Cells that are transformed with plasmids encoding surface display of streptavidin allow the 5'-biotin tagged aptamer to conjugate to the cell and the aptamer-cell complex to be utilized for a variety of therapeutic applications (fibrin clot degradation in this context). Additionally, the advancement and optimization of surface display of proteins, including streptavidin, will allow even more innovative synthetic biology approaches to develop. For example, a streptokinase releasing cell advances the relatively unexplored focus of synthetic biology in a cardiovascular setting. Lastly, addition of an Alexa 647 fluorophore to the 5'-end of ssDNA, also demonstrated by the dsDNA probe, creates the possibility of a fibrin-specific aptamer to emit a fluorescent signal at the site of a fibrin clot. Fluorophore quenchers and aptamer antidotes (ssDNA complementary to the aptamer sequence) have been used with DNA biosensors and could fine tune a fibrin biosensor used in vivo alongside current thrombus detection strategies. All in all, the continuation and optimization of the methods described in this work provides the opportunity for the identification and utilization of a fibrin-specific aptamer.

REFERENCES

[1] C. L. Ventola, "The nanomedicine revolution: Part 1: Emerging concepts," *P T: a peer-reviewed journal for formulary management*, vol. 37, pp. 512–525, 9 2012.

[2] R. Rajagopalan and J. V. Yakhmi, "Chapter 8 - nanotechnological approaches toward cancer chemotherapy," in *Nanostructures for Cancer Therapy*, ser. Micro and Nano Technologies, A. Ficai and A. M. Grumezescu, Eds., Elsevier, 2017, pp. 211–240, ISBN: 978-0-323-46144-3.

[3] H. Maeda, J. Wu, T. Sawa, Y. Matsumura, and K. Hori, "Tumor vascular permeability and the epr effect in macromolecular therapeutics: A review," pp. 271–284, 2000.

[4] E. Dotan, C. Aggarwal, and M. Smith, "Impact of rituximab (rituxan) on the treatment of b-cell non-hodkin's lymphoma," *Pharmacy and Therapeutics*, vol. 35, pp. 148–157, 3 2010.

[5] A. S. Wolberg, "Thrombin generation and fibrin clot structure," *Blood Reviews*, vol. 21, no. 3, pp. 131–142, 2007.

[6] L. Medved', O. Gorkun, and P. Privalov, "Structural organization of c-terminal parts of fibrinogen aî±-chains," *FEBS Letters*, vol. 160, no. 1-2, pp. 291–295, 1983.

[7] K. F. Standeven *et al.*, "Functional analysis of fibrin γ-chain cross-linking by activated factor xiii: Determination of a cross-linking pattern that maximizes clot stiffness," *Blood*, vol. 110, no. 3, pp. 902–907, 2007.

[8] S. Z. Goldhaber and N. Grasso-Correnti, "Treatment of blood clots," *Circulation*, vol. 106, no. 20, e138–e140, 2002.

[9] "Physiology, plasminogen activation," *StatPearls*, 2021.

[10] C. Kiparissides and O. Kammona, "Nanoscale carriers for targeted delivery of drugs and therapeutic biomolecules," *The Canadian Journal of Chemical Engineering*, vol. 91, no. 4, pp. 638–651, 2013.

[11] M. C. Johnston and C. J. Scott, "Antibody conjugated nanoparticles as a novel form of antibody drug conjugate chemotherapy," *Drug Discovery Today: Technologies*, vol. 30, pp. 63–69, 2018.

[12] K. H. Khan, "Gene expression in mammalian cells and its applications," *Advanced pharmaceutical bulletin*, vol. 3, no. 2, p. 257, 2013.

[13] H. Li, Y. Yang, W. Hong, M. Huang, M. Wu, and X. Zhao, "Applications of genome editing technology in the targeted therapy of human diseases: Mechanisms, advances and prospects," *Signal transduction and targeted therapy*, vol. 5, no. 1, pp. 1–23, 2020.

[14] F. D. Urnov, E. J. Rebar, M. C. Holmes, H. S. Zhang, and P. D. Gregory, "Genome editing with engineered zinc finger nucleases," *Nature Reviews Genetics*, vol. 11, no. 9, pp. 636–646, 2010.

[15] D. A. Wright, T. Li, B. Yang, and M. H. Spalding, "Talen-mediated genome editing: Prospects and perspectives," *Biochemical Journal*, vol. 462, no. 1, pp. 15–24, 2014.

[16] N. Savić and G. Schwank, "Advances in therapeutic crispr/cas9 genome editing," *Translational Research*, vol. 168, pp. 15–21, 2016.

[17] C. P. Paul, P. D. Good, I. Winer, and D. R. Engelke, "Effective expression of small interfering rna in human cells," *Nature biotechnology*, vol. 20, no. 5, pp. 505–508, 2002.

[18] M. D. Jansson and A. H. Lund, "Microrna and cancer," *Molecular Oncology*, vol. 6, no. 6, pp. 590–610, 2012, Cancer epigenetics.

[19] H. M. Weintraub, "Antisense rna and dna," *Scientific American*, vol. 262, no. 1, pp. 40–47, 1990.

[20] J. S. Mattick and I. V. Makunin, "Non-coding rna," *Human molecular genetics*, vol. 15, no. suppl_1, R17–R29, 2006.

[21] R. Lowe, N. Shirley, M. Bleackley, S. Dolan, and T. Shafee, "Transcriptomics technologies," *PLOS Computational Biology*, vol. 13, no. 5, pp. 1–23, May 2017.

[22] A. Zhang, H. Sun, P. Wang, Y. Han, and X. Wang, "Modern analytical techniques in metabolomics analysis," *Analyst*, vol. 137, no. 2, pp. 293–300, 2012.

[23] B. Merrifield, "Solid phase synthesis," *Science*, vol. 232, no. 4748, pp. 341–347, 1986.

[24] M. D. Matteucci and M. H. Caruthers, "Synthesis of deoxyoligonucleotides on a polymer support," *Journal of the American Chemical Society*, vol. 103, no. 11, pp. 3185–3191, 1981.

[25] S. Beaucage and M. Caruthers, "Deoxynucleoside phosphoramidites - a new class of key intermediates for deoxypolynucleotide synthesis," *Tetrahedron Letters*, vol. 22, no. 20, pp. 1859–1862, 1981.

[26] M. H. Caruthers, "The chemical synthesis of dna/rna: Our gift to science," *Journal of Biological Chemistry*, vol. 288, no. 2, pp. 1420–1427, 2013.

[27] J. H. Bauer and E. G. Pickels, "A high speed vacuum centrifuge suitable for the study of filterable viruses," *The Journal of Experimental Medicine*, vol. 64, no. 4, p. 503, 1936.

[28] F. Sanger, S. Nicklen, and A. R. Coulson, "Dna sequencing with chain-terminating inhibitors," *Proceedings of the National Academy of Sciences*, vol. 74, no. 12, pp. 5463–5467, 1977.

[29] N. S. Templeton, "The polymerase chain reaction. history, methods, and applications.," *Diagnostic molecular pathology: the American journal of surgical pathology, part B*, vol. 1, no. 1, pp. 58–72, 1992.

[30] L. Gold, "Selex: How it happened and where it will go," *Journal of Molecular Evolution*, vol. 81, pp. 140–143, 5.

[31] S. Burge, G. N. Parkinson, P. Hazel, A. K. Todd, and S. Neidle, "Quadruplex dna: Sequence, topology and structure," *Nucleic Acids Research*, vol. 34, no. 19, pp. 5402–5415, Sep. 2006.

[32] C. Tuerk and L. Gold, "Systematic evolution of ligands by exponential enrichment: Rna ligands to bacteriophage t4 dna polymerase," *science*, vol. 249, no. 4968, pp. 505–510, 1990.

[33] M. Avci-Adali, A. Paul, N. Wilhelm, G. Ziemer, and H. P. Wendel, "Upgrading selex technology by using lambda exonuclease digestion for single-stranded dna generation," *Molecules*, vol. 15, no. 1, pp. 1–11, 2009.

[34] M. J. N. Tapp, J. M. Slocik, P. B. Dennis, R. R. Naik, and V. T. Milam, "Competition-enhanced ligand selection to identify dna aptamers," *ACS Combinatorial Science*, vol. 20, no. 10, pp. 585–593, 2018. eprint: https://doi.org/10.1021/acscombsci.8b00048.

[35] K. Szeto *et al.*, "Rapid-selex for rna aptamers," *PloS one*, vol. 8, no. 12, e82667, 2013.

[36] M. Tapp, P. Dennis, R. R. Naik, and V. T. Milam, "Competition-enhanced ligand selection to screen for dna aptamers for spherical gold nanoparticles," *Langmuir*, vol. 37, no. 30, pp. 9043–9052, 2021. eprint: https://doi.org/10.1021/acs.langmuir.1c01053.

[37] Y. Ning, J. Hu, and F. Lu, "Aptamers used for biosensors and targeted therapy," *Biomedicine Pharmacotherapy*, vol. 132, p. 110 902, 2020.

[38] A. D. Keefe, S. Pai, and A. Ellington, "Aptamers as therapeutics," *Nature reviews Drug discovery*, vol. 9, no. 7, pp. 537–550, 2010.

[39] J. Rao, A. Dragulescu-Andrasi, and H. Yao, "Fluorescence imaging in vivo: Recent advances," *Current Opinion in Biotechnology*, vol. 18, no. 1, pp. 17–25, 2007, Analytical biotechnology.

[40] P. THEISEN, C. MCCOLLUM, K. UPADHYA, K. JACOBSON, H. VU, and A. ANDRUS, "Cheminform abstract: Fluorescent dye phosphoramidite labelling of oligonucleotides.," *ChemInform*, vol. 24, no. 2, p. 1, 1993.

[41] B. Powell Gray *et al.*, "Tunable cytotoxic aptamer–drug conjugates for the treatment of prostate cancer," *Proceedings of the National Academy of Sciences*, vol. 115, no. 18, pp. 4761–4766, 2018.

[42] C. M. Dundas, D. Demonte, and S. Park, "Streptavidin–biotin technology: Improvements and innovations in chemical and biological applications," *Applied microbiology and biotechnology*, vol. 97, no. 21, pp. 9343–9353, 2013.

[43] P. S. Stayton *et al.*, "Streptavidinâ€"biotin binding energetics," *Biomolecular Engineering*, vol. 16, no. 1, pp. 39–44, 1999.

[44] R. T. Pon, "A long chain biotin phosphoramidite reagent for the automated synthesis of 5â€²-biotinylated oligonucleotides," *Tetrahedron Letters*, vol. 32, no. 14, pp. 1715–1718, 1991.

[45] V. Thaore, D. Tsourapas, N. Shah, and C. Kontoravdi, "Techno-economic assessment of cell-free synthesis of monoclonal antibodies using cho cell extracts," *Processes*, vol. 8, no. 4, 2020.

[46] J. Zhou and J. Rossi, "Aptamers as targeted therapeutics: Current potential and challenges," *Nature reviews Drug discovery*, vol. 16, no. 3, pp. 181–202, 2017.

[47] R. Pasqualini and W. Arap, "Hybridoma-free generation of monoclonal antibodies," *Proceedings of the National Academy of Sciences*, vol. 101, no. 1, pp. 257–259, 2004.

[48] H. Sun, X. Zhu, P. Y. Lu, R. R. Rosato, W. Tan, and Y. Zu, "Oligonucleotide aptamers: New tools for targeted cancer therapy," *Molecular Therapy-Nucleic Acids*, vol. 3, e182, 2014.

[49] O. Antipova, E. Zavyalova, A. Golovin, G. Pavlova, A. Kopylov, and R. Reshetnikov, "Advances in the application of modified nucleotides in selex technology," *Biochemistry (Moscow)*, vol. 83, no. 10, pp. 1161–1172, 2018.

[50] Y. Lin, Q. Qiu, S. C. Gill, and S. D. Jayasena, "Modified rna sequence pools for in vitro selection," *Nucleic acids research*, vol. 22, no. 24, pp. 5229–5234, 1994.

[51] N. C. Pagratis *et al.*, "Potent 2-amino-, and 2-fluoro-2-deoxyribonucleotide rna inhibitors of keratinocyte growth factor," *Nature biotechnology*, vol. 15, no. 1, pp. 68–73, 1997.

[52] J. Ruckman *et al.*, "2-fluoropyrimidine rna-based aptamers to the 165-amino acid form of vascular endothelial growth factor (vegf165): Inhibition of receptor binding and vegf-induced vascular permeability through interactions requiring the exon 7-encoded domain," *Journal of Biological Chemistry*, vol. 273, no. 32, pp. 20 556–20 567, 1998.

[53] C. F. Earhart, "[30] use of an lpp-ompa fusion vehicle for bacterial surface display," in ser. Methods in Enzymology, vol. 326, Academic Press, 2000, pp. 506–516.

[54] M. Gustavsson, E. BÃ¤cklund, and G. Larsson, "Optimisation of surface expression using the aida autotransporter," *Microbial Cell Factories*, vol. 10, 1 2011.

[55] C. Yang *et al.*, "Cell surface display of functional macromolecule fusions on escherichia coli for development of an autofluorescent whole-cell biocatalyst," *Environmental Science Technology*, vol. 42, no. 16, pp. 6105–6110, 2008.

[56] T. Heinisch *et al.*, "E. coli surface display of streptavidin for directed evolution of an allylic deallylase," *Chemical Sciences*, vol. 9, pp. 5383–5388, 24 2018.

[57] M. Jeiranikhameneh, M. R. Razavi, S. Irani, S. D. Siadat, and M. Oloomi, "Designing novel construction for cell surface display of protein e on escherichia coli using non-classical pathway based on lpp-ompa," *AMB Express*, vol. 7, 1.

[58] T. Peschke, K. S. Rabe, and C. M. Niemeyer, "Orthogonal surface tags for whole-cell biocatalysis," *Angewandte Chemie International Edition*, vol. 56, no. 8, pp. 2183–2186,

[59] J. A. Francisco, C. F. Earhart, and G. Georgiou, "Transport and anchoring of beta-lactamase to the external surface of escherichia coli," *Proceedings of the National Academy of Sciences*, vol. 89, no. 7, pp. 2713–2717, 1992.

[60] M. Park, J. Jose, S. ThÃ¶mmes, J.-I. Kim, M.-J. Kang, and J.-C. Pyun, "Autodisplay of streptavidin," *Enzyme and Microbial Technology*, vol. 48, no. 4, pp. 307–311, 2011.

[61] S. M. Sedlak, L. C. Schendel, H. E. Gaub, and R. C. Bernardi, "Streptavidin/biotin: Tethering geometry defines unbinding mechanics," *Science Advances*, vol. 6, no. 13, eaay5999, 2020.

[62] M. I. Stefan and N. Le NovÃ¨re, "Cooperative binding," *PLOS Computational Biology*, vol. 9, pp. 1–6, Jun. 2013.

[63] J. Schultz *et al.*, "A tetravalent single-chain antibody-streptavidin fusion protein for pretargeted lymphoma therapy," *Cancer research*, vol. 60, no. 23, pp. 6663–6669, 2000.

[64] H. R. Nordlund, O. H. Laitinen, V. P. Hytönen, S. T. Uotila, E. Porkka, and M. S. Kulomaa, "Construction of a dual chain pseudotetrameric chicken avidin by combining two circularly permuted avidins," *Journal of Biological Chemistry*, vol. 279, no. 35, pp. 36 715–36 719, 2004.

[65] H. R. Nordlund *et al.*, "Tetravalent single-chain avidin: From subunits to protein domains via circularly permuted avidins," *Biochemical journal*, vol. 392, no. 3, pp. 485–491, 2005.

[66] M. Fairhead, D. Krndija, E. D. Lowe, and M. Howarth, "Plug-and-play pairing via defined divalent streptavidins," *Journal of Molecular Biology*, vol. 426, no. 1, pp. 199–214, 2014.

[67] M. Howarth *et al.*, "A monovalent streptavidin with a single femtomolar biotin binding site," *Nature methods*, vol. 3, no. 4, pp. 267–273, 2006.

[68] A. Banerjee, Y. Chisti, and U. Banerjee, "Streptokinase—a clinically useful thrombolytic agent," *Biotechnology advances*, vol. 22, no. 4, pp. 287–307, 2004.

[69] G. Murano, B. Wiman, and B. BlombÃ¤ck, "Human fibrinogen: Some characteristics of its s-carboxymethyl derivative chains," *Thrombosis Research*, vol. 1, no. 2, pp. 161–171, 1972.

[70] J. Jarmander, M. Gustavsson, T.-H. Do, P. Samuelson, and G. Larsson, "A dual tag system for facilitated detection of surface expressed proteins in escherichia coli," *Microbial cell factories*, vol. 11, no. 1, pp. 1–10, 2012.

[71] J. Zempleni, S. S. Wijeratne, and Y. I. Hassan, "Biotin," *Biofactors*, vol. 35, no. 1, pp. 36–46, 2009.

[72] K. Wakui *et al.*, "Rapidly neutralizable and highly anticoagulant thrombin-binding dna aptamer discovered by mace selex," *Molecular Therapy-Nucleic Acids*, vol. 16, pp. 348–359, 2019.

[73] L. C. Bock, L. C. Griffin, J. A. Latham, E. H. Vermaas, and J. J. Toole, "Selection of single-stranded dna molecules that bind and inhibit human thrombin," *nature*, vol. 355, no. 6360, pp. 564–566, 1992.

[74] D. M. Tasset, M. F. Kubik, and W. Steiner, "Oligonucleotide inhibitors of human thrombin that bind distinct epitopes," *Journal of molecular biology*, vol. 272, no. 5, pp. 688–698, 1997.

[75] E. Y. Savchik *et al.*, "Aptamer ra36 inhibits of human, rabbit, and rat plasma coagulation activated with thrombin or snake venom coagulases," *Bulletin of experimental biology and medicine*, vol. 156, no. 1, pp. 44–48, 2013.

[76] C. P. Rusconi *et al.*, "Rna aptamers as reversible antagonists of coagulation factor ixa," *Nature*, vol. 419, no. 6902, pp. 90–94, 2002.